A regularized high-order moment model to capture non-Maxwellian electron energy distribution function effects in partially ionized plasmas

Alejandro Alvarez Laguna, B. Esteves, A. Bourdon, P. Chabert

A regularized high-order moment model to capture non-Maxwellian electron energy distribution function effects in partially-ionized plasmas

A. Alvarez Laguna,[1, a)] B. Esteves,[1] A. Bourdon,[1] and P.Chabert[1]

Laboratoire de Physique des Plasmas, CNRS, Ecole Polytechnique, 91128, Palaiseau, France

(*Electronic mail: alvarez@lpp.polytechnique.fr)

(Dated: 23 August 2022)

A model for electrons in partially-ionized plasmas that self-consistently captures non-Maxwellian electron energy distribution function (EEDF) effects is presented. The model is based on the solution of scalar and vectorial velocity moments up to the contracted fourth-order moment. The set of fluid (macroscopic) equations is obtained with Grad's method and exact expressions for the collision production terms are derived, considering the electron-electron, electron-gas, and electron-ion elastic collisions as well as for electron-gas excitation and ionization collisions. A regularization of the equations is proposed in order to avoid spurious discontinuities, existing in the original Grad's moment model, by using a generalized Chapman-Enskog expansion that exploits the disparity of mass between the electrons and the heavy particles (ions and atoms) as well as the disparity of plasma and gas densities, typical of gas discharges. The transport model includes non-local effects due to spatial gradients in the EEDF as well as the impact of the EEDF in the calculation of the elastic and inelastic collision rates. Solutions of the moment model under spatially-homogeneous conditions are compared to direct simulation Monte-Carlo (DSMC) and a two-term Boltzmann solver under conditions that are representative of high plasma density discharges at low-pressure. The moment model is able to self-consistently capture the evolution of the EEDF, in good quantitative agreement with the kinetic solutions. The calculation of transport coefficients and collision rates of an argon plasma in thermal non-equilibrium under the effect of an electric field are in good agreement with the solutions of a two-term Boltzmann solver, largely improving models with a simplified Bhatnagar–Gross–Krook (BGK) collisional operator.

[a)]Corresponding author

I. INTRODUCTION

Electrons in partially-ionized plasmas often do not follow a Maxwellian distribution due to the collisions with a much colder gas, spatial inhomogeneities, and the presence of electromagnetic fields[1,2]. Fluid models for the electrons in partially-ionized plasmas usually solve for the first few moments of the Boltzmann equation of the electrons, i.e., the continuity equation, the momentum equation (often in the drift-diffusion approximation), and the energy equation, e.g.[3–7]. However, these equations include transport coefficients and reaction rates that depend on the electron energy distribution function.

In gas discharges, the transport coefficients and the reaction rates for electron fluid models are often obtained by solving the spatially homogeneous electron kinetic equation in the two-term approximation[8,9]. This approach expands the distribution function into spherical harmonics[10,11] and solves for the evolution equations for the isotropic part and the anisotropy in the direction of the first spherical harmonic, while the anisotropy is assumed to be small as compared to the spherical part of the distribution function. The resulting coefficients are then put into lookup tables as a function of the local electron mean energy[12,13] or as a function of the local reduced electric field[14,15]. Even though the mean-energy approximation considers a non-local electron energy equation, the transport and rate coefficients are computed from the solution of a Boltzmann solver that assumes a local equilibrium between electric acceleration and collisional momentum and energy losses under spatially-homogeneous conditions, as in the local-field approximation. However, the local approximation is not justified in the low-pressure regime where the electron energy relaxation length can become comparable to the length of the spatial inhomogeneities and, consequently, the spatial gradients need to be taken into account in the kinetic equation[16,17].

Standalone fluid models for the electrons are used to study high plasma density ($10^{16} - 10^{19}$ m^{-3}) discharges at low pressure (< 50 mTorr)[18–20]. Altough fluid models under these conditions are compromised by the fact that the electron-electron mean-free path is comparable to the size of the device, the dimensions of the system are often too large for full kinetic simulations. These fluid models do not use the transport coefficients from the Boltzmann solver as the local approximation is no longer valid. Instead, most of these multi-fluid models, e.g.[18–20], obtain the closure by taking moments of a kinetic equation with a Bhatnagar–Gross–Krook (BGK) operator for the electron-neutral collisions where the collisional frequency is computed as an average rate computed with Maxwellian electrons. As it will be shown in this paper, the resulting system of fluid equations

is incomplete (missing effects such as thermal friction or the effect of non-Maxwellian electron energy distribution function (EEDF)) and overestimates the transport coefficients and collisional rates, in particular the ionization and excitation rates.

Alternatively, in order to account for non-equilibrium processes, some authors have proposed to solve the equations for higher-order moments. In addition to density, momentum, and energy conservation, Refs.[20–23] include the equation for the electron heat flux. Zielke et al.[20] and Futtersack[23] proposed a simplified equation for the heat flux with a closure that is obtained by assuming a Maxwellian EEDF for the closure fluxes of the heat flux equation while neglecting the inertial terms and a BGK operator for the elastic collisions with the gas. Alternatively, Dujko et al.[22,24] compute the collision terms of the moment model with collision rates computed through the multi-term Boltzmann equation using the momentum transfer theory while the closure flux of the quartic tensor is based on a adjustable parameter. Becker & Loffhagen[21] propose a model that obtains the closure for the heat flux equation that relies on the local approximation, i.e., the transport fluxes and collisional rates are tabulated from the solution of a Boltzmann solver. Some of these high-order moment models were studied and compared by Garland et al.[25]

In this paper, we will derive from the kinetic equation a non-linear model that is based on the Grad's method[26–28]. This work follows the methodology that has been used in other non-equilibrium problems such as rarified gases[29,30], granular gases[31] or electrons in semiconductors[32,33]. In our model, the collision frequencies, the closure fluxes, and the transport coefficients are analytically derived by taking moments of the Boltzmann collisional operator with the non-Maxwellian distribution function and are function of the macroscopic variables. Thus, as opposed to the above-mentioned models, the closure does not rely on the local approximation, does not contains adjustable coefficients and does not use a simplified BGK collisional term.

Grad's models have been studied in fully-ionized plasmas[34–36] and partially-ionized plasmas[37]. In the classical works[34,35,37], in addition to the plasmadynamical moments (mass, momentum, and energy for each particle species), the authors consider vectorial and tensorial moments. In addition, the authors study the linear regime of the moment system. In this regime, the transport fluxes are obtained by solving a linear system of equations. As we will show in this paper, with this choice of moments (i.e., vectorial and second-rank tensorial), these models do not study perturbations in the electron energy distribution function (EEDF), and, therefore, cannot capture the depletion of the electron population at high density, characteristic of gas discharges. For this reason, we propose a moment method that studies the evolution of moments that are responsible for the isotropic (scalar

moments) and first anisotropy (vectorial moments) of the distribution function, which allows for self-consistently capturing non-Maxwellian EEDFs. The relation between the Hermitian moment expansion and the multi-term Boltzmann solver is discussed in detail in a number of references in the context of electron swarms and gas discharges[11,38–41].

Grad's moment model equations are known to have mathematical problems (see, e.g., refs.[27,30,42]). The fluxes of Grad's moment set of equations are written exclusively as a function of the macroscopic variables $F(\mathbf{U})$, as in hyperbolic systems. This results in spurious discontinuities, problems at the boundaries, and, in general, problems to solve numerically the equations[27,30]. Struchtrup & Torrilhon[29,30] have proposed a method for the regularization of the equations in neutral gases that consists in adding parabolic terms in the fluxes, i.e., $F(\mathbf{U}, \nabla\mathbf{U})$. This terms are derived from a Chapman-Enskog expansion considering the equations of high-order moments[43]. This regularization yields solutions that are smooth and stable as opposed to Grad's equations, Burnett or super-Burnett equations. In the present work, we will also regularize Grad's equations by adding parabolic terms that are obtained through a Chapman-Enskog expansion that exploits the smallness of the electron mass and the disparity of plasma and gas densities, typical of gas discharges.

In this work, we present the derivation of the system of equations that solves for the scalar and vectorial moments up to the contracted fourth moment (density, momentum, energy, heat-flux and contracted fourth-moment, which in 3D results in 9 scalar equations), called in the following 9-M model. We determine the collision terms of the 9-M equations by taking moments of the full Boltzmann collision operator, including electron-heavy (ions and gas) and electron-electron elastic collisions and electron-gas inelastic and ionization collisions. In addition, we will regularize the system of equations by considering a transport model that simplifies the momentum and heat-flux equations when the anisotropic part of the electron velocity distribution function is small as compared to the isotropic part, which is justified by the presence of electron-gas collisions.

In order to validate the collisional integrals and transport coefficients of our model, we compare the solution of our model to kinetic simulations, both direct simulation Monte-Carlo (DSMC) and to a two-term Boltzmann solver, under spatially-homogeneous conditions with conditions that are representative of gas discharges at low-pressure and high-plasma density.

The plan of the paper is as follows. First, we present the electron kinetic equation and the equation of transfer. Second, we present the 9-M Grad's moment model equations. Third, we determine the collision terms for the moment system. Fourth, we propose a regularization of the equations based on a Chapman-Enskog expansion that exploits the electron-heavy mass ratio

and the ionization degree. Finally, we compare spatially-homogeneous solutions of the model to kinetic simulations.

II. ELECTRON KINETIC EQUATION AND GENERAL TRANSPORT EQUATION

A. Electron kinetic equation

The electron kinetic equation describes the evolution of the electron distribution in the phase space, as follows,

$$\frac{\partial f_{\mathfrak{e}}}{\partial t} + \boldsymbol{v}\cdot\nabla f_{\mathfrak{e}} - \frac{e\boldsymbol{E}}{m_{\mathfrak{e}}}\cdot\nabla_{\boldsymbol{v}} f_{\mathfrak{e}} = \left.\frac{\delta f_{\mathfrak{e}}}{\delta t}\right|_c . \tag{1}$$

Here, $\boldsymbol{E}$ is the electric field, $m_{\mathfrak{e}}$ is the electron mass, and e is the elementary charge. We consider the electron collisional processes that are the dominant collisions in a low-pressure non-equilibrium plasma in an atomic gas. We consider the elastic collisions with heavy species (neutral gas and ions), elastic collisions with electrons, excitation collisions with the gas and electron impact ionization collisions. As a result, the collisional term of the kinetic equation reads

$$\left.\frac{\delta f_{\mathfrak{e}}}{\delta t}\right|_c = \sum_{\alpha}^{\mathfrak{i},\mathfrak{g}} \left.\frac{\delta f_{\mathfrak{e}}}{\delta t}\right|_{\mathfrak{e}\alpha}^{el} + \left.\frac{\delta f_{\mathfrak{e}}}{\delta t}\right|_{\mathfrak{e}\mathfrak{e}}^{el} + \left.\frac{\delta f_{\mathfrak{e}}}{\delta t}\right|_{\mathfrak{e}\mathfrak{g}}^{exc} + \left.\frac{\delta f_{\mathfrak{e}}}{\delta t}\right|_{\mathfrak{e}\mathfrak{g}}^{iz}, \tag{2}$$

where the subscripts $\mathfrak{e}$, $\mathfrak{i}$, and $\mathfrak{g}$ stands for the electron, ion, and gas species, respectively.

1. Elastic collisions

In this work, we consider a Boltzmann operator for the elastic collisions, as follows,

$$\left.\frac{\delta f_{\mathfrak{e}}}{\delta t}\right|_{\mathfrak{e}\alpha}^{el} = \int\int \left(f'_{\mathfrak{e}} f'_{\alpha} - f_{\mathfrak{e}} f_{\alpha}\right) g\,\sigma_{\mathfrak{e}\alpha} d\Omega d\boldsymbol{v}_{\alpha}, \tag{3}$$

where the prime corresponds to the distribution after the collision, α is the subindex for the target species (neutral, ions, and electrons), $d\Omega$ is the solid angle element of the deflected particle in the center of mass reference frame, $g = |\boldsymbol{v}_{\mathfrak{e}} - \boldsymbol{v}_{\alpha}|$ is the modulus of the relative velocity between the colliding particles, and $\sigma_{\mathfrak{e}\alpha}(g,\Omega)$ is the differential cross-section of the interaction.

In elastic collisions of the type, $\mathfrak{e} + \alpha \rightarrow \mathfrak{e} + \alpha$, the collision conserves the momentum and the energy, as follows,

$$m_{\mathfrak{e}}\boldsymbol{v}_{\mathfrak{e}} + m_{\alpha}\boldsymbol{v}_{\alpha} = m_{\mathfrak{e}}\boldsymbol{v}'_{\mathfrak{e}} + m_{\alpha}\boldsymbol{v}'_{\alpha} \quad \text{and} \quad \frac{1}{2}m_{\mathfrak{e}}v_{\mathfrak{e}}^2 + \frac{1}{2}m_{\alpha}v_{\alpha}^2 = \frac{1}{2}m_{\mathfrak{e}}v_{\mathfrak{e}}'^2 + \frac{1}{2}m_{\alpha}v_{\alpha}'^2. \tag{4}$$

In the calculation of the rates and transport coefficients, we use effective cross sections integrated over the angles[37,44], as follows,

$$Q^{(l)}_{\alpha\beta}(g) = 2\pi \int_0^{\pi} \left(1-\cos^l\chi\right) \sigma_{\alpha\beta}(g,\chi)\sin\chi d\chi, \tag{5}$$

where $l=1$ is the momentum-transfer (or diffusion) cross section.

We consider a Coulomb potential screened at the Debye length for the electron-ion and electron-electron collisions[37] which yields the following momentum-transfer and viscosity cross sections

$$Q^{(1)}_{\mathfrak{e}\alpha}(g) = 2\pi b_0^2 \ln\left[1+\left(\frac{r_D}{b_0}\right)^2\right] \text{ and } Q^{(2)}_{\mathfrak{e}\alpha}(g) = 4\pi b_0^2 \left\{\ln\left[1+\left(\frac{r_D}{b_0}\right)^2 - \frac{\left(\frac{r_D}{b_0}\right)^2}{1+\left(\frac{r_D}{b_0}\right)^2}\right]\right\}, \tag{6}$$

where $b_0 = e^2/(2\pi\varepsilon_0\mu_{\mathfrak{e}\alpha}g^2)$, the reduced mass $\mu_{\mathfrak{e}\alpha} = m_{\mathfrak{e}}m_\alpha/(m_{\mathfrak{e}}+m_\alpha)$, the Debye length $r_D^2 = \varepsilon_0 T_{\mathfrak{e}}/(n_{\mathfrak{e}}e)$ and ε_0 is the vacuum permittivity. Note that this collisional term is formally different from the Fokker-Planck collision model that is usually used in the two-term approximation[4]. Nevertheless, as noted in refs.[37,45], this model provides similar results to the Landau collision operator.

2. Inelastic and ionization collisions

We consider excitation collisions of the type, $\mathfrak{e}+\mathfrak{g} \xrightarrow{\phi^*} \mathfrak{e}+\mathfrak{g}^*$, where ϕ^* is the excitation energy. In this work, we do not follow the excited states of the gas, and we consider all the gas states as a single species. The Boltzmann operator for excitation collisions reads,

$$\left.\frac{\delta f_{\mathfrak{e}}}{\delta t}\right|^{exc}_{\mathfrak{e}\mathfrak{g}} = \int\int \left(f'_{\mathfrak{e}}f'_{\mathfrak{g}} - f_{\mathfrak{e}}f_{\mathfrak{g}}\right) g\,\sigma^{exc}_{\mathfrak{e}\mathfrak{g}} d\Omega d\boldsymbol{v}_{\mathfrak{g}}. \tag{7}$$

In this case, the relation between the pre-collisional and post-collisional velocities are related by

$$m_{\mathfrak{e}}\boldsymbol{v}_{\mathfrak{e}} + m_{\mathfrak{g}}\boldsymbol{v}_{\mathfrak{g}} = m_{\mathfrak{e}}\boldsymbol{v}'_{\mathfrak{e}} + m_{\mathfrak{g}}\boldsymbol{v}'_{\mathfrak{g}} \quad \text{and} \quad \frac{1}{2}m_{\mathfrak{e}}v_{\mathfrak{e}}^2 + \frac{1}{2}m_{\mathfrak{g}}v_{\mathfrak{g}}^2 = \frac{1}{2}m_{\mathfrak{e}}v_{\mathfrak{e}}'^2 + \frac{1}{2}m_{\mathfrak{g}}v_{\mathfrak{g}}'^2 + e\phi^*. \tag{8}$$

We define the following transport cross-section for the inelastic collisions, as described by Robson[11],

$$Q^{(l)}_{\alpha\beta}(g) = 2\pi\int_0^{\pi}\left[1-\left(\frac{g'}{g}\cos\chi\right)^l\right]\sigma_{\alpha\beta}(g,\chi)\sin\chi d\chi, \text{ and } Q^{(T)}_{\alpha\beta}(g) = 2\pi\int_0^{\pi}\sigma_{\alpha\beta}(g,\chi)\sin\chi d\chi, \tag{9}$$

where, g'/g is the ratio of the relative velocities after and before the collision.

We consider the ionization process $\mathfrak{e}+\mathfrak{g} \xrightarrow{\phi^{iz}} \mathfrak{e}+\mathfrak{e}+\mathfrak{i}$ where ϕ^{iz} is the ionization energy and we neglect the recombination, as usually done in Boltzmann solvers[8], since the plasma density is much smaller than the gas density. The Boltzmann operator for the ionization collision reads[38],

$$\left.\frac{\delta f_\mathfrak{e}}{\delta t}\right|_{\mathfrak{eg}}^{iz} = \int\int 2 f_{\mathfrak{e}_1}^\star f_\mathfrak{g}^\star g_{\mathfrak{eg}}^\star \sigma_{\mathfrak{eg}}^{iz\star} \frac{d\boldsymbol{v}_{\mathfrak{e}_1}^\star}{d\boldsymbol{v}_\mathfrak{e}} d\Omega d\boldsymbol{v}_\mathfrak{g}^\star - \int\int f_\mathfrak{e} f_\mathfrak{g} g_{\mathfrak{eg}} \sigma_{\mathfrak{eg}}^{iz} d\Omega d\boldsymbol{v}_\mathfrak{g}, \tag{10}$$

where the factor 2 of the restitution collision (i.e., positive term) is the stoichiometry coefficient. In this case, the relation between the pre-collisional $(\boldsymbol{v}_\mathfrak{e}^\star, \boldsymbol{v}_\mathfrak{g}^\star)$ and post-collisional $(\boldsymbol{v}_{\mathfrak{e}_1}, \boldsymbol{v}_{\mathfrak{e}_2}, \boldsymbol{v}_\mathfrak{i})$ velocities are related by

$$m_\mathfrak{e}\boldsymbol{v}_\mathfrak{e}^\star + m_\mathfrak{g}\boldsymbol{v}_\mathfrak{g}^\star = m_\mathfrak{e}\boldsymbol{v}_{\mathfrak{e}_1} + m_\mathfrak{e}\boldsymbol{v}_{\mathfrak{e}_2} + m_\mathfrak{i}\boldsymbol{v}_\mathfrak{i} \quad \text{and} \quad \frac{1}{2}m_\mathfrak{e}v_\mathfrak{e}^{\star 2} + \frac{1}{2}m_\mathfrak{g}v_\mathfrak{g}^{\star 2} = \frac{1}{2}m_\mathfrak{e}v_{\mathfrak{e}_1}^2 + \frac{1}{2}m_\mathfrak{e}\boldsymbol{v}_{\mathfrak{e}_2}^2 + \frac{1}{2}m_\mathfrak{i}v_\mathfrak{i}^2 + e\phi^{iz}. \tag{11}$$

The definition of the transport cross-sections for inelastic collisions, as shown in Eq. (9), will also be used for the ionization collisions.

B. General transport equation

We consider the transport equation in a reference frame moving at the electron mean velocity. This equation is obtained by averaging the kinetic equation multiplied by a weight ψ that is a function of the velocity $\boldsymbol{v}$ over the velocity space. We define the peculiar velocity, $\boldsymbol{c}_\mathfrak{e} = \boldsymbol{v} - \boldsymbol{u}_\mathfrak{e}$, where $\boldsymbol{u}_\mathfrak{e}$ is the electron mean velocity, defined as

$$\boldsymbol{u}_\mathfrak{e} = \frac{1}{n_\mathfrak{e}}\int \boldsymbol{v} f_\mathfrak{e} d\boldsymbol{v} \quad \text{with} \quad n_\mathfrak{e} = \int f_\mathfrak{e} d\boldsymbol{v}. \tag{12}$$

The general transport equation reads[37]

$$\frac{\partial}{\partial t}\int f_\mathfrak{e}\psi d\boldsymbol{c}_\mathfrak{e} + \nabla\cdot\int f_\mathfrak{e}\psi(\boldsymbol{c}_\mathfrak{e}+\boldsymbol{u}_\mathfrak{e})d\boldsymbol{c}_\mathfrak{e} - \int f_\mathfrak{e}\boldsymbol{F}_\mathfrak{e}^*\cdot\nabla_{\boldsymbol{c}_\mathfrak{e}}\psi d\boldsymbol{c}_\mathfrak{e} + \int f_\mathfrak{e} c_{\mathfrak{e}_i}\frac{\partial\psi}{\partial c_{\mathfrak{e}_j}}\frac{\partial u_{\mathfrak{e}_j}}{\partial x_i}d\boldsymbol{c}_\mathfrak{e} = \int\psi\left.\frac{\delta f_\mathfrak{e}}{\delta t}\right|_c d\boldsymbol{c}_\mathfrak{e}, \tag{13}$$

where, the forces in the non-inertial reference frame read

$$n_\mathfrak{e}\boldsymbol{F}_\mathfrak{e}^* = -en_\mathfrak{e}\boldsymbol{E} - m_\mathfrak{e}n_\mathfrak{e}\left(\frac{\partial}{\partial t} + \boldsymbol{u}_\mathfrak{e}\cdot\nabla\right)\boldsymbol{u}_\mathfrak{e}. \tag{14}$$

III. A MOMENT MODEL WITH NON-MAXWELLIAN EEDF

A. The Grad's method and the relation with the multi-term Boltzmann approximation

In order to close the fluxes and the collisional terms of the system of moment equations, Grad's method assumes that the non-equilibrium distribution function is a perturbed Maxwellian distribution, as follows,

$$f_{\mathfrak{e}}(\boldsymbol{x},\boldsymbol{c}_{\mathfrak{e}},t) = f_{\mathfrak{e}}^{(0)}(\boldsymbol{x},c_{\mathfrak{e}},t)[1+\chi_{\mathfrak{e}}(\boldsymbol{c}_{\mathfrak{e}})], \tag{15}$$

where the Maxwellian distribution function reads

$$f_{\mathfrak{e}}^{(0)}(\boldsymbol{x},c_{\mathfrak{e}},t) = n_{\mathfrak{e}}\left(\frac{\beta_{\mathfrak{e}}}{\pi}\right)^{3/2} e^{-\beta_{\mathfrak{e}}c_{\mathfrak{e}}^2} \quad \text{with} \quad \beta_{\mathfrak{e}} = \frac{m_{\mathfrak{e}}}{2eT_{\mathfrak{e}}}. \tag{16}$$

The perturbation is written as an expansion in Hermite polynomials, which in the case of irreducible polynomials[35] reads

$$\chi_{\mathfrak{e}}(\boldsymbol{c}_{\mathfrak{e}}) = \sum_{n=0}^{N} h^{(2n)}H^{(2n)}(\boldsymbol{c}_{\mathfrak{e}}) + \sum_{n=0}^{M} h_r^{(2n+1)}H_r^{(2n+1)}(\boldsymbol{c}_{\mathfrak{e}}) + \sum_{n=0}^{P} h_{rs}^{(2n)}H_{rs}^{(2n)}(\boldsymbol{c}_{\mathfrak{e}}) + \cdots, \tag{17}$$

where we use the Einstein notation. Here, $h^{(2n)}$, $h_r^{(2n+1)}$, $h_{rs}^{(2n)}$... are coefficients that are written as a function of the macroscopic variables and hence each term of the expansion is related to the resolution of a macroscopic moment equation. $H^{(2n)}$, $H_r^{(2n+1)}$, $H_{rs}^{(2n)}$... are the irreducible Hermite polynomials of order n where $H^{(2n)}$ correspond to the scalar polynomials, $H_r^{(2n+1)}$ are vectorial, and $H_{rs}^{(2n)}$ are second-rank tensors. N, M, P... are the number of polynomials of each type that are considered in the expansion.

The use of this expansion to solve the kinetic equation in multi-term Boltzmann discretization is detailed in refs.[11,38–41] Similarly, Balescu[35] points out the correspondence between the irreducible Hermite polynomials and the expansion in Laguerre-Sonine polynomials and spherical harmonics. The perturbation in the polynomials $H^{(2n)}$ is responsible for the isotropic part of the distribution function, $H_r^{(2n+1)}$ for the perturbations in the direction of the first spherical harmonic, $H_{rs}^{(2n)}$ for the perturbations in the direction of the second spherical harmonic, etcetera.

In classical works in plasma physics such as refs.[34,35,37], the perturbation of the distribution function is chosen along the first and second spherical harmonic. Similarly, 13-M moment models for rarefied gases[27,29] solve for moments in these directions of the velocity space. Alternatively, in this paper, we consider a model that considers perturbations in the same directions of the two-term Boltzmann approach, i.e., an expansion in $H^{(2n)}$ and $H_r^{(2n+1)}$. For this reason, in addition to mass,

momentum and energy, we consider the heat-flux vector, which relates to $h_r^{(3)}$, in order to capture perturbations in the first spherical harmonics, and the contracted fourth moment, related to $h^{(4)}$, in order to capture perturbations in the isotropic part.

B. Grad's 9-M equations

The 9-M equations are obtained by considering the following weights in the transport equation, i.e., Eq. (13),

$$\boldsymbol{\psi} = \left(1,\ m_{\mathfrak{e}}\boldsymbol{v},\ \frac{m_{\mathfrak{e}}}{2}c_{\mathfrak{e}}^2,\ \frac{m_{\mathfrak{e}}}{2}c_{\mathfrak{e}}^2\boldsymbol{c}_{\mathfrak{e}},\ \frac{m_{\mathfrak{e}}}{2}c_{\mathfrak{e}}^4\right)^T. \tag{18}$$

As a result, the macroscopic state of the electrons is characterized by nine scalar fields: particle density $n_{\mathfrak{e}}$, mean velocity $\boldsymbol{u}_{\mathfrak{e}}$, isotropic pressure $p_{\mathfrak{e}}$, heat-flux vector $\boldsymbol{q}_{\mathfrak{e}}$, and the scalar contracted fourth moment $p_{\mathfrak{e}_{iijj}}$, where the subindices i, j refer to the directions following the Einstein notation. These fields are defined as follows,

$$\begin{gathered} n_{\mathfrak{e}} = \int f_{\mathfrak{e}} d\boldsymbol{v}, \quad \rho_{\mathfrak{e}} u_{\mathfrak{e}_i} = \int m_{\mathfrak{e}} v_i f_{\mathfrak{e}} d\boldsymbol{v}, \quad p_{\mathfrak{e}} = \frac{1}{3}\int m_{\mathfrak{e}} c_{\mathfrak{e}}^2 f_{\mathfrak{e}} d\boldsymbol{v}, \\ q_{\mathfrak{e}_i} = \frac{1}{2}\int m_{\mathfrak{e}} c_{\mathfrak{e}}^2 c_{\mathfrak{e}_i} f_{\mathfrak{e}} d\boldsymbol{v}, \quad \text{and} \quad p_{\mathfrak{e}_{iijj}} = \frac{1}{2}\int m_{\mathfrak{e}} c_{\mathfrak{e}}^4 f_{\mathfrak{e}} d\boldsymbol{v}. \end{gathered} \tag{19}$$

By using the transport equation, we obtain the following system of equations,

$$\frac{\partial n_{\mathfrak{e}}}{\partial t} + \frac{\partial}{\partial x_i} n_{\mathfrak{e}} u_{\mathfrak{e}_i} = \dot{n}_{\mathfrak{e}}, \tag{20}$$

$$m_{\mathfrak{e}}\frac{\partial}{\partial t} n_{\mathfrak{e}} u_{\mathfrak{e}_i} + \frac{\partial}{\partial x_j}\left(m_{\mathfrak{e}} n_{\mathfrak{e}} u_{\mathfrak{e}_i} u_{\mathfrak{e}_j} + p_{\mathfrak{e}}\delta_{ij}\right) = -e n_{\mathfrak{e}} E_i + R_i, \tag{21}$$

$$\frac{3}{2}\frac{\partial p_{\mathfrak{e}}}{\partial t} + \frac{\partial}{\partial x_k}\left(q_{\mathfrak{e}_k} + \frac{3}{2}p_{\mathfrak{e}} u_{\mathfrak{e}_k}\right) + p_{\mathfrak{e}}\frac{\partial u_{\mathfrak{e}_k}}{\partial x_k} = Q, \tag{22}$$

$$\begin{aligned} \frac{\partial q_{\mathfrak{e}_i}}{\partial t} + \frac{\partial}{\partial x_j}\left(r_{\mathfrak{e}_{ij}} + q_{\mathfrak{e}_i} u_{\mathfrak{e}_j}\right) + r_{\mathfrak{e}_{ijk}}\frac{\partial u_{\mathfrak{e}_k}}{\partial x_j} + q_{\mathfrak{e}_j}\frac{\partial u_{\mathfrak{e}_i}}{\partial x_j} \\ - \frac{5}{2}\frac{p_{\mathfrak{e}}}{\rho_{\mathfrak{e}}}\frac{\partial p_{\mathfrak{e}}}{\partial x_j}\delta_{ij} = R_i^{hf} - \frac{5}{2}\frac{p_{\mathfrak{e}}}{\rho_{\mathfrak{e}}}\left(R_i - m_{\mathfrak{e}}\dot{n}_{\mathfrak{e}} u_{\mathfrak{e}_i}\right), \end{aligned} \tag{23}$$

$$\begin{aligned} \frac{\partial}{\partial t} p_{\mathfrak{e}_{iijj}} + \frac{\partial}{\partial x_k}\left(r_{\mathfrak{e}_{iijjk}} + p_{\mathfrak{e}_{iijj}} u_{\mathfrak{e}_k}\right) + 4 r_{\mathfrak{e}_{ij}}\frac{\partial u_{\mathfrak{e}_i}}{\partial x_j} \\ - 4\frac{q_{\mathfrak{e}_i}}{\rho_{\mathfrak{e}}}\frac{\partial p_{\mathfrak{e}}}{\partial x_j}\delta_{ij} = Q^{(4)} - 4\frac{q_{\mathfrak{e}_i}}{\rho_{\mathfrak{e}}}\left(R_i - m_{\mathfrak{e}}\dot{n}_{\mathfrak{e}} u_{\mathfrak{e}_i}\right). \end{aligned} \tag{24}$$

We define the normalized contracted fourth-moment that measures the deviations of the fourth-order moment from a Maxwellian,

$$\Delta_{\mathfrak{e}} = \frac{p_{\mathfrak{e}_{iijj}} - \frac{15}{2}\frac{n_{\mathfrak{e}} e^2 T_{\mathfrak{e}}^2}{m_{\mathfrak{e}}}}{\frac{15}{2}\frac{n_{\mathfrak{e}} e^2 T_{\mathfrak{e}}^2}{m_{\mathfrak{e}}}}. \tag{25}$$

Note that Δ_e represents the excess kurtosis of the distribution function. We define the electron temperature (in eV) from the mean internal energy by considering an ideal gas law, as follows,

$$T_e = \frac{1}{3n_e e}\int m_e c_e^2 f_e d\boldsymbol{v} = \frac{p_e}{n_e e}. \tag{26}$$

In Eqs. (23) and (24), the fluxes that appear in the equations are defined as

$$r_{e_{ijk}} = \frac{1}{2}\int m_e c_{e_i} c_{e_j} c_{e_k} f_e d\boldsymbol{v}, \quad r_{e_{ij}} = \frac{1}{2}\int m_e c_e^2 c_{e_i} c_{e_j} f_e d\boldsymbol{v}, \text{ and } r_{e_{iijjk}} = \frac{1}{2}\int m_e c_e^4 c_{e_k} f_e d\boldsymbol{v}. \tag{27}$$

These fluxes will be computed with the expression of the Grad's distribution function. Additionally, the right-hand-side of the equations contains the collisional terms, i.e., $\dot{n}_e$, $\boldsymbol{R}$, Q, $\boldsymbol{R}^{hf}$, and $Q^{(4)}$, which will be derived in the next section.

C. Grad's non-equilibrium distribution function and closure fluxes

The Grad's non-equilibrium distribution function for this choice of moments reads

$$f_e^{(9M)}(\boldsymbol{x}, \boldsymbol{c}_e, t) = f_e^{(0)}(\boldsymbol{x}, c_e, t)\left[1 + \chi_{isot}^{(9M)}(\boldsymbol{c}) + \chi_{anisot}^{(9M)}(\boldsymbol{c})\right] \tag{28}$$

where

$$\chi_{isot}^{(9M)}(\boldsymbol{c}_e) = \sum_{n=0}^{2} h^{(2n)} H^{(2n)}(c_e) = \left(\frac{15}{8} - \frac{5\beta_e}{2}c_e^2 + \frac{\beta_e^2}{2}c_e^4\right)\Delta_e$$

and

$$\chi_{anisot}^{(9M)}(\boldsymbol{c}_e) = \sum_{n=0}^{1} h_r^{(2n+1)} H_r^{(2n+1)}(c_e) = \frac{8\beta_e^2}{5\rho_e} q_{e_i} c_{e_i}\left(\beta_e c_e^2 - \frac{5}{2}\right).$$

The non-equilibrium distribution function can be easily computed from the definition of the moments[35].

The closure fluxes are obtained by introducing the distribution function into Eq. (27). The explicit expressions of the transport fluxes for this closure read

$$r_{e_{ijk}} = \frac{2}{5}\left(q_{e_i}\delta_{jk} + q_{e_j}\delta_{ik} + q_{e_k}\delta_{ij}\right), \quad r_{e_{ij}} = \frac{5}{2}\frac{p_e^2}{\rho_e}\left(1+\Delta_e\right)\delta_{ij}, \quad \text{and} \quad r_{e_{iijjk}} = 14\frac{p_e}{\rho_e}q_{e_k}. \tag{29}$$

In the following, it will be useful to define the EEDF of the Grad's 9-M model to study the evolution of the distribution function in the energy space. The EEDF is defined as $g_e d\mathscr{E}_e = c_e^2 dc_e \int f_e d\Omega_{\boldsymbol{v}_e}$ where the energy in eV is $\mathscr{E}_e = m_e c_e^2/(2e)$. In the case of the 9-M model, the EEDF reads,

$$\begin{aligned} g_e^{(9M)}(\boldsymbol{x}, \mathscr{E}_e, t) &= \frac{1}{2}\left(\frac{2e}{m_e}\right)^{3/2} \mathscr{E}_e^{1/2} \int f_e(\boldsymbol{x}, \boldsymbol{c}_e(\mathscr{E}_e, \Omega_{\boldsymbol{v}_e}), t) d\Omega_{\boldsymbol{v}_e} \\ &= \frac{2n_e}{T_e\sqrt{\pi}}\left(\frac{\mathscr{E}_e}{T_e}\right)^{1/2} e^{-\frac{\mathscr{E}_e}{T_e}}\left[1 + \frac{15}{8}\Delta_e - \frac{5}{2}\left(\frac{\mathscr{E}_e}{T_e}\right)\Delta_e + \frac{1}{2}\left(\frac{\mathscr{E}_e}{T_e}\right)^2\Delta_e\right]. \end{aligned} \tag{30}$$

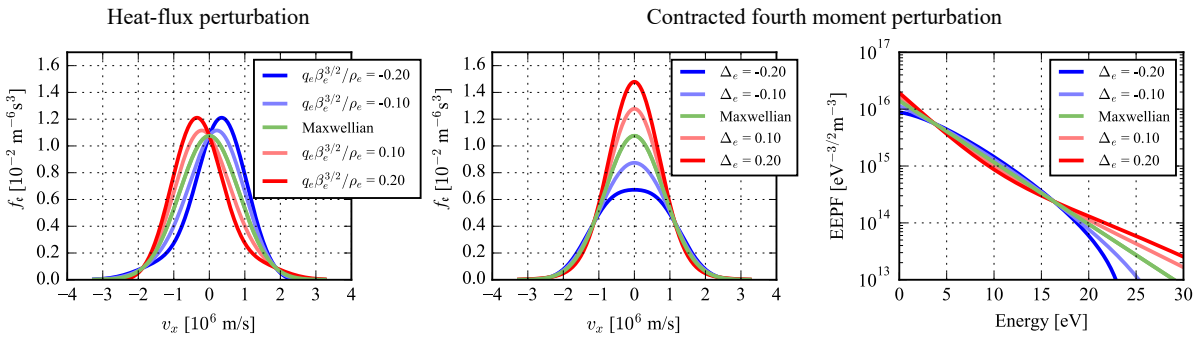

FIG. 1. Left panel: Effect of a perturbation in the heat flux on the electron distribution function in the velocity space. Center panel: Effect of a contracted fourth-moment perturbation on the distribution function in the velocity space. Right panel: effect of a contracted fourth-moment perturbation on the electron energy probability function (EEPF). The distribution functions are computed for fixed values of $T_e = 4$ eV and $n_e = 10^{17}$ m^{-3}.

Sometimes, in order to quatify the distribution function in the energy space, the electron probability function (EEPF) is used instead the EEDF. The EEPF is simply computed as $g_p^{(9M)}(\boldsymbol{x}, \mathscr{E}_e, t) = \mathscr{E}_e^{-1/2} g_e^{(9M)}(\boldsymbol{x}, \mathscr{E}_e, t)$. Note that, in semi-log scale, the EEPF of a Maxwellian as a function of the energy is a straight line. For this reason, the EEPF allows to easily identify non-Maxwellian distribution functions in the energy space.

In Fig. 1, we illustrate the effect of the heat-flux vector and normalized contracted fourth-moment in the distribution function. The heat-flux vector is a result of a perturbation in the symmetry of the distribution function. In statistics, this perturbation in the symmetry is usually referred to as skewness. On the other hand, the contracted fourth moment is a result of a perturbation in the tails of the distribution function, which in statistics is referred to as kurtosis of the distribution function. The perturbations in the fourth-moment allows for representing non-Maxwellian distribution functions in the energy space, as shown in Fig. 1. As it can be seen, $\Delta_e < 0$ corresponds to Druyvesteyn-like distribution functions with a depopulated tail at high energies. Alternatively, $\Delta_e > 0$ corresponds to two-temperature like distributions with two different slopes at low and high energies.

As presented in Fig. 2, the Grad's 9-M non-equilibrium distribution function can represent the EEDF in low-pressure discharges in a noble gas. In Fig. 2, we present an example of the experimental measurements by Aanesland et al.[46] of the EEDFs in a low-pressure inductively-coupled plasma (ICP) discharge, operating without magnetic filter with argon at 10 mTorr and

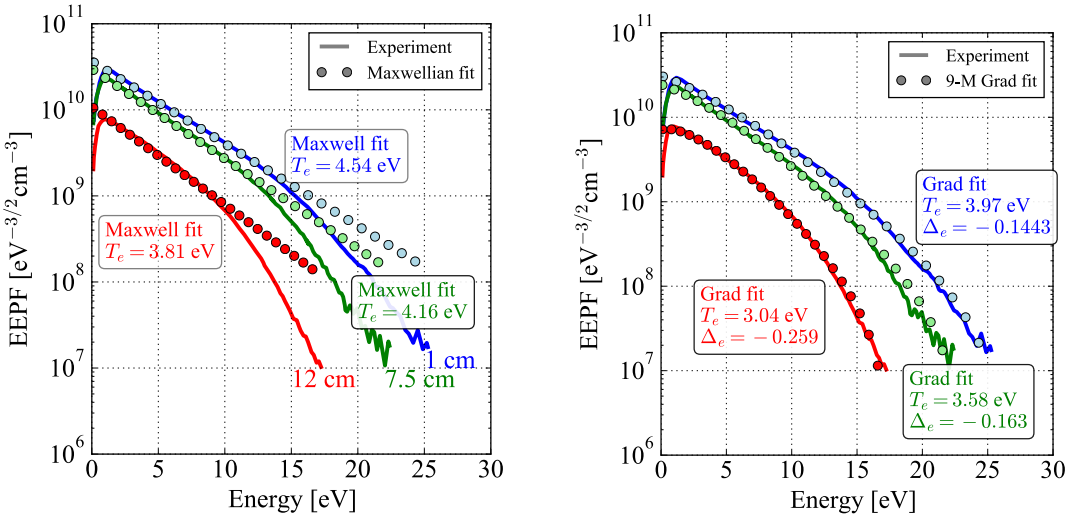

FIG. 2. Experimental measurements (solid lines) of the EEPF for an argon ICP discharge at 10 mTorr and 130 W, reproduced from Aanesland et al.[46], Appl. Phys. Lett. 100, 044102 (2012), with the permission of AIP Publishing. The measurements are taken at 1 cm (blue), 7.5 cm (green), and 12 cm (red) from the antenna that produces the inductive heating. We fit (circles) the experimental results with a Maxwellian (left) and a 9-M Grad's function (right). The 9-M Grad EEPF captures the shape of the experimental EEDFs.

power of 130 W. The measurements are presented at three different distances from the RF antenna that generates the plasma. We fit the experimental EEPFs with a Maxwellian and a Grad 9-M distribution functions. The results show that the Grad 9-M can better capture the shape of the EEPF both at high-energies (in the inelastic range, i.e., for energies above the first excitation potential) and low-energies (in the elastic range, for energies below the excitation potential). Note that the maximum at low energies of the experimental EEPFs is an artifact of the Langmuir probe measurements that are not able to collect all the electrons at low energies[47]. Consequently, the actual EEPF under the measured conditions should present the maximum at $\mathscr{E}_\epsilon = 0$, as in the Grad 9-M fit. In addition, we can see that the normalized fourth moment Δ_ϵ is a quantity that varies along the axis of the discharge due to the non-local transport. The values of Δ_ϵ that were found in the fit are negative as the distribution function is depleted at high energies.

IV. DETERMINATION OF THE COLLISION TERMS

We compute the collisional source terms that appear in Eqs. (20)-(24) as the moment of the collisional operator in the kinetic equation, with the weights of Eq. (18), as follows,

$$\int \psi_{\mathfrak{e}} \left.\frac{\delta f_{\mathfrak{e}}}{\delta t}\right|_c d\boldsymbol{v} = \int \begin{pmatrix} 1 \\ m_{\mathfrak{e}}\boldsymbol{v} \\ \frac{m_{\mathfrak{e}}}{2}c_{\mathfrak{e}}^2 \\ \frac{m_{\mathfrak{e}}}{2}c_{\mathfrak{e}}^2\boldsymbol{c}_{\mathfrak{e}} \\ \frac{m_{\mathfrak{e}}}{2}c_{\mathfrak{e}}^4 \end{pmatrix} \left.\frac{\delta f_{\mathfrak{e}}}{\delta t}\right|_c d\boldsymbol{v} = \begin{pmatrix} \dot{n}_{\mathfrak{e}} \\ \boldsymbol{R} \\ Q \\ \boldsymbol{R}^{hf} \\ Q^{(4)} \end{pmatrix}, \tag{31}$$

where the collisional operators for the elastic, inelastic and ionization collisions are presented in Eqs. (3), (7), and (10). As usually done in the two-term Boltzmann solvers for low-temperature plasmas, we consider the neutral gas and the ions, i.e., $\alpha \in (\mathrm{i},\ \mathfrak{g})$, to be a Maxwellian at a different temperature than electrons, i.e.,

$$f_\alpha^{(M)}(\boldsymbol{x},\boldsymbol{v}_\alpha,t) = n_\alpha \left(\frac{\beta_\alpha}{\pi}\right)^{3/2} \exp\left(-\beta_\alpha v_\alpha^2\right) \quad \text{with} \quad \beta_\alpha = \frac{m_\alpha}{2eT_\alpha}. \tag{32}$$

By introducing the Grad's distribution function of Eq. (28), the integral of Eq. (31) can be resolved analytically. The computation of the collisional integrals for a multi-species plasma is far from being trivial. Nevertheless, the exact analytical expressions can be obtained in the case of Grad's method. In this work, we computed the integrals assisted by a computer algebra code written in the python library SymPy[48].

A. Electron-gas and electron-ion elastic collisions

We use the reciprocity relations of the elastic collision (c.f., Eq. (3.28) in ref.[27]) to write the moment of the elastic collisional operator Eq. (3), as follows,

$$\int \psi_{\mathfrak{e}} \left.\frac{\delta f_{\mathfrak{e}}}{\delta t}\right|_{\mathfrak{e}\alpha}^{el} d\boldsymbol{v} = \int\int\int (\psi'_{\mathfrak{e}} - \psi_{\mathfrak{e}}) f_{\mathfrak{e}} f_\alpha g \sigma d\Omega d\boldsymbol{v}_\alpha d\boldsymbol{v}_{\mathfrak{e}}, \tag{33}$$

where $\alpha \in (\mathrm{i},\mathfrak{g})$.

The integral of the collisional operator will be performed in the inertial reference frame with a change of the integration variables by replacing the velocities $\boldsymbol{v}_{\mathfrak{e}}$ and $\boldsymbol{v}_\alpha$ by the relative velocity $\boldsymbol{g}$ and the velocity of the center of mass $\boldsymbol{G}$, that are defined as follows,

$$\boldsymbol{G} = \frac{m_{\mathfrak{e}}\boldsymbol{v}_{\mathfrak{e}} + m_\alpha \boldsymbol{v}_\alpha}{m_{\mathfrak{e}} + m_\alpha}, \quad \boldsymbol{g} = \boldsymbol{v}_{\mathfrak{e}} - \boldsymbol{v}_\alpha. \tag{34}$$

The linear momentum conservation implies that $\boldsymbol{G}' = \boldsymbol{G}$ and the conservation of energy $g = g'$, so the pre-collisional and post-collisional velocities in the center of mass variables read

$$\boldsymbol{v}_\mathfrak{e} = \boldsymbol{G} + \frac{\mu_{\mathfrak{e}\alpha}}{m_\mathfrak{e}}\boldsymbol{g} \quad \boldsymbol{v}_\alpha = \boldsymbol{G} - \frac{\mu_{\mathfrak{e}\alpha}}{m_\alpha}\boldsymbol{g}, \quad \boldsymbol{v}'_\mathfrak{e} = \boldsymbol{G} + \frac{\mu_{\mathfrak{e}\alpha}}{m_\mathfrak{e}}\boldsymbol{g}' \quad \text{and} \quad \boldsymbol{v}'_\alpha = \boldsymbol{G} - \frac{\mu_{\mathfrak{e}\alpha}}{m_\alpha}\boldsymbol{g}', \tag{35}$$

where the reduced mass is defined as $\mu_{\mathfrak{e}\alpha} = m_\mathfrak{e} m_\alpha/(m_\mathfrak{e} + m_\alpha)$.

We can write $\boldsymbol{g}'$ as a function of $\boldsymbol{g}$ and the scattering angles[37] and integrate the collision unit sphere as follows,

$$\int \psi_\mathfrak{e} \left.\frac{\delta f_\mathfrak{e}}{\delta t}\right|_{\mathfrak{e}\alpha}^{el} d\boldsymbol{v}_\mathfrak{e} = -\mu_{\mathfrak{e}\alpha} \int\int \mathscr{F}_{\mathfrak{e}\alpha}^{el}(\boldsymbol{g}, \boldsymbol{G}) f_\mathfrak{e} f_\alpha g d\boldsymbol{g} d\boldsymbol{G}. \tag{36}$$

where $\mathscr{F}_{\mathfrak{e}\alpha}^{el}(\boldsymbol{g}, \boldsymbol{G})$ for the first five moments is presented in Appendix A 1.

In order to perform the analytical integration, we need to perform another change of variables as the electrons and the heavy species have a different temperature. We define the new variable

$$\tilde{\boldsymbol{G}} = \boldsymbol{G} + \frac{\mu_{\mathfrak{e}\alpha}}{\beta_T}\left(\frac{\beta_\mathfrak{e}}{m_\mathfrak{e}} - \frac{\beta_\alpha}{m_\alpha}\right)\boldsymbol{g}, \quad \text{with} \quad \beta_T = \beta_\mathfrak{e} + \beta_\alpha, \text{ and } \beta_{\mathfrak{e}\alpha} = \frac{\beta_\mathfrak{e}\beta_\alpha}{\beta_T}. \tag{37}$$

With this new variable, the multiplication between the two distribution functions reads,

$$f_\mathfrak{e} f_\alpha = n_\mathfrak{e} n_\alpha \left(\frac{\beta_T}{\pi}\right)^{3/2} \left(\frac{\beta_{\mathfrak{e}\alpha}}{\pi}\right)^{3/2} e^{-\beta_T \tilde{G}^2} e^{-\beta_{\mathfrak{e}\alpha} g^2} (1 + \chi_\mathfrak{e}), \tag{38}$$

where $\chi_\mathfrak{e}$ needs to be expressed as a function of the new variables $(\tilde{\boldsymbol{G}}, \boldsymbol{g})$. In this work, we consider cases where the electron velocity is much smaller than the electron thermal speed, i.e., $u_\mathfrak{e}^2 \ll \beta_\mathfrak{e}^{-1}$.

The integration of the integrals in Eq. (36) can be done with the table 6.1 of ref.[35] and are verified with a computer algebra code. In the following results, we neglect the terms of order $\mathscr{O}(u_\mathfrak{e}^2 \beta_\mathfrak{e})$ or smaller.

Once the integrals are solved, as the results are solved in the inertial frame, we write the collisional source terms in the non-inertial reference frame, moving at $\boldsymbol{u}_\mathfrak{e}$ through the relations of Eq. (A5) in Appendix A 2.

The electron-heavy elastic collisional source terms read

$$\left.\begin{pmatrix} \dot{n}_\mathfrak{e} \\ \boldsymbol{R} \\ Q \\ \boldsymbol{R}^{hf} \\ Q^{(4)} \end{pmatrix}\right|_{\mathfrak{e}\alpha}^{el} = \begin{pmatrix} 0 \\ -m_\mathfrak{e} n_\mathfrak{e} \nu_{\mathfrak{e}\alpha}^{(u,1)} \boldsymbol{u}_\mathfrak{e} - m_\mathfrak{e} n_\mathfrak{e} \nu_{\mathfrak{e}\alpha}^{(q,1)} \frac{\boldsymbol{q}_\mathfrak{e}}{p_\mathfrak{e}} \\ -\frac{m_\mathfrak{e}}{m_\alpha} n_\mathfrak{e} \nu_{\mathfrak{e}\alpha}^{(T,2)} e\,(T_\mathfrak{e} - T_\alpha) - \frac{m_\mathfrak{e}}{m_\alpha} n_\mathfrak{e} \nu_{\mathfrak{e}\alpha}^{(\Delta,2)} \Delta_\mathfrak{e} e T_\alpha + m_\mathfrak{e} n_\mathfrak{e} \nu_{\mathfrak{e}\alpha}^{(u,1)} u_\mathfrak{e}^2 + m_\mathfrak{e} n_\mathfrak{e} \nu_{\mathfrak{e}\alpha}^{(q,1)} \frac{\boldsymbol{q}_\mathfrak{e}}{p_\mathfrak{e}} \cdot \boldsymbol{u}_\mathfrak{e} \\ -n_\mathfrak{e} \nu_{\mathfrak{e}\alpha}^{(u,3)} e T_\mathfrak{e} \boldsymbol{u}_\mathfrak{e} - \nu_{\mathfrak{e}\alpha}^{(q,3)} \boldsymbol{q}_\mathfrak{e} \\ -\frac{m_\mathfrak{e}}{m_\alpha} \nu_{\mathfrak{e}\alpha}^{(T,4)} \frac{p_\mathfrak{e}^2}{\rho_\mathfrak{e}} \left(1 - \frac{T_\alpha}{T_\mathfrak{e}}\right) - \frac{m_\mathfrak{e}}{m_\alpha} \nu_{\mathfrak{e}\alpha}^{(\Delta,4)} \Delta_\mathfrak{e} \frac{p_\mathfrak{e}^2}{\rho_\mathfrak{e}} \frac{T_\alpha}{T_\mathfrak{e}} + 4 n_\mathfrak{e} \nu_{\mathfrak{e}\alpha}^{(u,3)} e T_\mathfrak{e} u_\mathfrak{e}^2 + 4 \nu_{\mathfrak{e}\alpha}^{(q,3)} \boldsymbol{q}_\mathfrak{e} \cdot \boldsymbol{u}_\mathfrak{e} \end{pmatrix}. \tag{39}$$

The collisional frequencies, which are proportional to the heavy particle density, read

$$\nu_{\mathfrak{e}\alpha}^{(u,1)} = \frac{16}{3} n_\alpha \Omega_{\mathfrak{e}\alpha}^{(1,1)},\ \nu_{\mathfrak{e}\alpha}^{(q,1)} = \frac{16}{3} n_\alpha \left[\frac{2}{5}\Omega_{\mathfrak{e}\alpha}^{(1,2)} - \Omega_{\mathfrak{e}\alpha}^{(1,1)}\right], \tag{40}$$

$$\nu_{\mathfrak{e}\alpha}^{(T,2)} = n_\alpha \left[(16+30\Delta_\mathfrak{e})\Omega_{\mathfrak{e}\alpha}^{(1,1)} - 40\Delta_\mathfrak{e}\Omega_{\mathfrak{e}\alpha}^{(1,2)} + 8\Delta_\mathfrak{e}\Omega_{\mathfrak{e}\alpha}^{(1,3)}\right], \tag{41}$$

$$\nu_{\mathfrak{e}\alpha}^{(u,3)} = \frac{16}{3} n_\alpha \Omega_{\mathfrak{e}\alpha}^{(1,2)},\ \ \nu_{\mathfrak{e}\alpha}^{(q,3)} = \frac{16}{3} n_\alpha \left[\frac{2}{5}\Omega_{\mathfrak{e}\alpha}^{(1,3)} - \Omega_{\mathfrak{e}\alpha}^{(1,2)}\right], \tag{42}$$

$$\nu_{\mathfrak{e}\alpha}^{(T,4)} = 2n_\alpha \left[(32+60\Delta_\mathfrak{e})\Omega_{\mathfrak{e}\alpha}^{(1,2)} - 80\Delta_\mathfrak{e}\Omega_{\mathfrak{e}\alpha}^{(1,3)} + 16\Delta_\mathfrak{e}\Omega_{\mathfrak{e}\alpha}^{(1,4)}\right] \tag{43}$$

$$\nu_{\mathfrak{e}\alpha}^{(\Delta,2)} = 16n_\alpha \left[\Omega_{\mathfrak{e}\alpha}^{(1,2)} - \frac{5}{2}\Omega_{\mathfrak{e}\alpha}^{(1,1)}\right],\quad \nu_{\mathfrak{e}\alpha}^{(\Delta,4)} = 64n_\alpha \left[\Omega_{\mathfrak{e}\alpha}^{(1,3)} - \frac{5}{2}\Omega_{\mathfrak{e}\alpha}^{(1,2)}\right] \tag{44}$$

In the expressions of the frequencies, we use the generalized Chapman-Cowling integrals[44] that represent the integration of the cross-section over the energy of the collisions and are defined as

$$\Omega_{\mathfrak{e}\alpha}^{(l,r)}(T_\mathfrak{e}) = \frac{1}{2}\left(\frac{1}{\pi\beta_\mathfrak{e}}\right)^{1/2} \int_0^\infty \xi^{2r+3} e^{-\xi^2} Q_{\mathfrak{e}\alpha}^{(l)} d\xi \quad \text{with} \quad \xi = \sqrt{\beta_\mathfrak{e}} g. \tag{45}$$

Note that the electron-gas energy relaxation frequency of Eq. (41) depends on the normalized fourth moment. This effect represent non-Maxwellian EEDF effects in the electron-gas energy exchange, which are usually neglected in fluid models.

B. Electron-gas inelastic and ionization collisions

As done above, we will first compute the source terms in the inertial reference frame and we will use the variables that were defined in Eq. (34). The same relations as in the elastic collisions holds, except for the energy conservation relation. In the ionization collisions, we consider that the secondary electron is created at the same energy as the primary electrons (equal sharing hypothesis). As a result, the energy conservation for excitation and ionization collisions read, respectively,

$$\frac{\mu_{\mathfrak{eg}}}{2} g^2 = \frac{\mu_{\mathfrak{eg}}}{2} g'^2 + e\phi^* \quad \text{and} \quad \frac{\mu_{\mathfrak{eg}}}{2} g^2 = \mu_{\mathfrak{eg}} g'^2 + e\phi^{iz}. \tag{46}$$

The reciprocity relation of Eq. (33) still holds in the case of inelastic and ionization collisions. The moment of the collisional operator reads

$$\int \psi_\mathfrak{e} \left.\frac{\delta f_\mathfrak{e}}{\delta t}\right|_{\mathfrak{eg}}^{iz,inel} d\boldsymbol{v} = \int\int\int (\psi'_\mathfrak{e} - \psi_\mathfrak{e}) f_\mathfrak{e} f_\mathfrak{g} g \sigma d\Omega d\boldsymbol{v}_\alpha d\boldsymbol{v}_\mathfrak{e} =$$
$$-\mu_{\mathfrak{eg}} \int\int \left[\mathscr{F}_{\mathfrak{eg}}^{el}(\boldsymbol{g},\boldsymbol{G}) + \mathscr{F}_{\mathfrak{eg}}^{inel,iz}(\boldsymbol{g},\boldsymbol{G})\right] f_\mathfrak{e} f_\mathfrak{g} g d\boldsymbol{g} d\boldsymbol{G}. \tag{47}$$

The integral over the scattering angles can be divided into two contributions, the first one that is identical to the one derived for the elastic collisions, Eq. (A1), and another contribution that depends on the energy loss of the excitation/ionization collisions. This integral over the scattering angles is presented in Eq. (A3) in Appendix A 1.

In order to tackle the integration of Eq. (47), we follow the same procedure as in the electron-heavy elastic collisions. First, we perform the change of variables of Eq. (37), after, we neglect the terms of order $\mathscr{O}(u_{\mathfrak{e}}^2\beta_{\mathfrak{e}})$ or smaller, and finally, we change the reference frame, as expressed in Eqs. (A5).

As seen in the collisional integral of Eq. (47), the inelastic and ionization collisional source terms have two contributions. The first has the same expression to the elastic collisions of Eq. (39) with the momentum transfer cross-section of the inelastic and ionization process. However, this contribution is in general smaller as the elastic collision frequency is larger than the inelastic or ionization ones. The second contribution, depends on the energy loss by the electron during the collision, as follows,

$$\left.\begin{pmatrix} \dot{n}_{\mathfrak{e}} \\ \boldsymbol{R} \\ Q \\ \boldsymbol{R}^{hf} \\ Q^{(4)} \end{pmatrix}\right|_{\mathfrak{eg}}^{inel,iz} = \sum_{k=0}^{excit,iz} \begin{pmatrix} n_{\mathfrak{e}} n_{\mathfrak{g}} K_{iz}^{(0)} \\ 0 \\ -n_{\mathfrak{e}} n_{\mathfrak{g}} K_k^{(0)} e\phi_k^* \\ \frac{5}{3}\boldsymbol{u}_{\mathfrak{e}} n_{\mathfrak{e}} n_{\mathfrak{g}} K_k^{(0)} e\phi_k^* \\ -2n_{\mathfrak{g}} \left(\frac{p_{\mathfrak{e}}^2}{\rho_{\mathfrak{e}}}\right) \left(2K_k^{(1)} \left(\frac{\phi_k^*}{T_e}\right) - K_k^{(0)} \left(\frac{\phi_k^*}{T_e}\right)^2\right) \end{pmatrix}. \tag{48}$$

The rate coefficients depend on the integral of the isotropic part of the distribution function, as follows,

$$K_{inel}^{(r)} = 4\pi \left(\frac{m_{\mathfrak{e}}}{2eT_{\mathfrak{e}}}\right)^r \int_0^\infty v_e^{2r+3} Q_{\mathfrak{eg}}^{(T)} f_{\mathfrak{e}}^{(0)} \left(1 + \chi_{isot}^{(9M)}\right) dv_{\mathfrak{e}}. \tag{49}$$

This integral depends on the temperature, density, and fourth-moment of the distribution function. One should note that for large negative normalized fourth-moments, i.e., $\Delta_{\mathfrak{e}} < -0.2$ a small part of the tail of the distribution function can become negative. This negative tail has negligible impact in the elastic collisions as the polynomial is multiplied by an exponential. However, it can produce an error in the computation of the inelastic rate coefficients. For this reason, in the current work we perform an numerical integration of the integral of Eq. (49) by only considering the positive part of the distribution function. In Fig. 3, we show the influence of the fourth moment in the ionization rate coefficient for the argon ionization cross section[49]. For negative values of $\Delta_{\mathfrak{e}}$ (which corresponds to a distribution function that is depopulated at high energies), the ionization

rate coefficient is much smaller than the one computed for a Maxwellian distribution function. Alternatively, positive values of Δ_e produce a larger ionization rate coefficient than the Maxwellian distribution function.

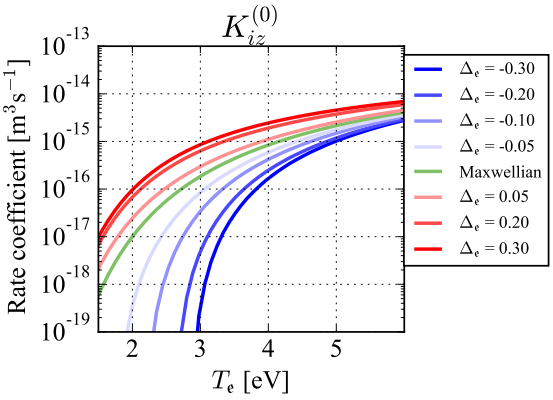

FIG. 3. Influence of the contracted fourth moment on the ionization rate coefficient $K_{iz}^{(0)}$ for argon.

C. Electron-electron elastic collisions

We use the reciprocity relation to write the moment of the electron-electron collisional operator, as follows,

$$\int \psi_e \left.\frac{\delta f_e}{\delta t}\right|_{ee}^{el} d\boldsymbol{v} = \frac{1}{2}\int\int\int (\psi_e' + \psi_{e_1}' - \psi_e - \psi_{e_1}) f_e f_{e_1} g \sigma d\Omega d\boldsymbol{v}_{e_1} d\boldsymbol{v}_e. \tag{50}$$

In this case, we perform the integrals in the reference frame moving at the electrons mean velocity. In this frame, we introduce the following variables

$$\boldsymbol{c}_e = \boldsymbol{G} + \frac{1}{2}\boldsymbol{g} \quad \boldsymbol{c}_{e_1} = \boldsymbol{G} - \frac{1}{2}\boldsymbol{g}, \quad \boldsymbol{c}_e' = \boldsymbol{G} + \frac{1}{2}\boldsymbol{g}' \quad \text{and} \quad \boldsymbol{c}_{e_1}' = \boldsymbol{G} - \frac{1}{2}\boldsymbol{g}'. \tag{51}$$

Here, $\boldsymbol{g} = \boldsymbol{c}_e - \boldsymbol{c}_{e_1}$ and $\boldsymbol{G} = 1/2(\boldsymbol{c}_e + \boldsymbol{c}_{e_1})$.

The integral over the scattering angles reads

$$\int \psi_e \left.\frac{\delta f_e}{\delta t}\right|_c d\boldsymbol{v}_e = \frac{m_e}{2}\int\int \mathscr{F}_{ee}^{el}(\boldsymbol{g},\boldsymbol{G}) f_e f_{e_1} g d\boldsymbol{g} d\boldsymbol{G}. \tag{52}$$

where $\mathscr{F}_{ee}^{el}(\boldsymbol{g},\boldsymbol{G})$ for the first five moments is presented in Eq. (A4) of Appendix A 1.

The multiplication of the two distribution function is approximated as follows

$$f_e f_{e_1} = f_e^{(0)} f_{e_1}^{(0)} (\chi_e + \chi_{e_1}), \tag{53}$$

where we neglect the non-linear terms.

The electron-electron elastic collisions conserve mass, momentum and energy for the electron species. Therefore, the collisional source terms have contributions to the heat flux and the contracted fourth moment relaxation, as follows

$$\left.\begin{pmatrix} \dot{n}_\mathfrak{e} \\ \boldsymbol{R} \\ Q \\ \boldsymbol{R}^{hf} \\ Q^{(4)} \end{pmatrix}\right|_{\mathfrak{e}\mathfrak{e}}^{el} = \begin{pmatrix} 0 \\ 0 \\ 0 \\ -\nu^q_{\mathfrak{e}\mathfrak{e}}\boldsymbol{q}_\mathfrak{e} \\ -\nu^\Delta_{\mathfrak{e}\mathfrak{e}}\frac{p^2_\mathfrak{e}}{\rho_\mathfrak{e}}\Delta_\mathfrak{e} \end{pmatrix}. \tag{54}$$

The relaxation frequencies are computed as

$$\nu^q_{\mathfrak{e}\mathfrak{e}} = \frac{16}{15} n_\mathfrak{e} \Omega^{(2,2)}_{\mathfrak{e}\mathfrak{e}}, \quad \text{and} \quad \nu^\Delta_{\mathfrak{e}\mathfrak{e}} = 8 n_\mathfrak{e} \Omega^{(2,2)}_{\mathfrak{e}\mathfrak{e}}, \tag{55}$$

where the integral of the cross-section over the energies reads

$$\Omega^{(2,2)}_{\mathfrak{e}\mathfrak{e}}(T_\mathfrak{e}) = \frac{1}{2}\left(\frac{2}{\pi\beta_\mathfrak{e}}\right)^{1/2} \int_0^\infty \xi^7 e^{-\xi^2} Q^{(2)}_{\mathfrak{e}\mathfrak{e}} d\xi \quad \text{with} \quad \xi = \sqrt{\beta_\mathfrak{e}/2} g. \tag{56}$$

V. REGULARIZED EQUATIONS: TRANSPORT MODEL FOR SMALL ANISOTROPIES IN THE ELECTRON VELOCITY DISTRIBUTION FUNCTION

The numerical resolution of Grad's moment equations yields fundamental problems that are related to the mathematical structure of the equations. The system of Eqs. (20)-(24) can be written as

$$\frac{\partial \mathbf{U}}{\partial t} + \mathbf{A}\frac{\partial \mathbf{U}}{\partial x} = \mathbf{S}. \tag{57}$$

This hyperbolic structure of the system of equations can lead to spurious discontinuities and problems in the boundary conditions[27,32].

A possible fix to this problem relies on a regularization of the equations that consists in adding parabolic terms, i.e., second-order spatial and/or mixed derivative to the system. The first attempt to derive the moment equations, including the parabolic terms, based on the order of accuracy in the Knudsen number was proposed by Müller et al.[43] In our work, we will follow the method proposed by Struchtrup & Torrilhon[29,30]. They proposed a regularization of the moment model by a Chapman-Enskog expansion of the macroscopic variables in series of the Knudsen number

(see, e.g., Chapter 7 of the monograph by Struchtrup[27]). In their work, they propose to expand the pressure deviator and the heat flux vector. Magin et al.[50,51] extended this procedure to multi-component plasmas. However, our case is fundamentally different as the electron heavy mass ratio appears in the normalized equations and the Knudsen numbers of the electron-gas and electron-electron are different because the ionization degree is usually small in gas discharges.

A. Normalized equations

We use the following normalization that considers the electron velocity is of the order of Bohm's speed and the heat flux of the order of the advection of energy at that speed, as follows,

$$\hat{n}_\mathfrak{e} = n_\mathfrak{e}/n_\mathfrak{e}^0, \quad \hat{\boldsymbol{u}}_\mathfrak{e} = \frac{\boldsymbol{u}_\mathfrak{e}}{\sqrt{eT_\mathfrak{e}^0/m_i}}, \quad \hat{T}_\mathfrak{e} = T_\mathfrak{e}/T_\mathfrak{e}^0, \quad \hat{\boldsymbol{q}}_\mathfrak{e} = \frac{\boldsymbol{q}_\mathfrak{e}}{p_\mathfrak{e}^0\sqrt{eT_\mathfrak{e}^0/m_i}}, \quad \hat{p}_{\mathfrak{e}_{iijj}} = \frac{p_{\mathfrak{e}_{iijj}}}{p_\mathfrak{e}^{0^2}/(m_\mathfrak{e} n_\mathfrak{e}^0)},$$

$$\hat{\boldsymbol{E}} = \boldsymbol{E}L^0/T_\mathfrak{e}^0, \quad \hat{x} = x/L^0, \quad \hat{t} = t\sqrt{eT_\mathfrak{e}/m_i}/L^0.$$

Here, $n_\mathfrak{e}^0$ and $T_\mathfrak{e}^0$, are the reference electron density and temperature, respectively, that are characteristic values of the conditions of the discharge. The reference pressure is computed as $p_\mathfrak{e}^0 = n_\mathfrak{e}^0 eT_\mathfrak{e}^0$. The reference length L^0 is taken to be a characteristic macroscopic length related to the size of the system of study. We normalize the collision frequencies to reference collision frequencies, as follows

$$\hat{\nu}_{\mathfrak{e}\mathfrak{h}} = \nu_{\mathfrak{e}\mathfrak{h}}/\nu_{\mathfrak{e}\mathfrak{h}}^0, \quad \hat{\nu}_{\mathfrak{e}\mathfrak{e}} = \nu_{\mathfrak{e}\mathfrak{e}}/\nu_{\mathfrak{e}\mathfrak{e}}^0, \quad \hat{\nu}_{\mathfrak{e}\mathfrak{g}}^{inel} = n_\mathfrak{g} K_{inel}^{(r)}/\nu_{\mathfrak{e}\mathfrak{g}}^{inel,0}, \quad \hat{\nu}_{\mathfrak{e}\mathfrak{g}}^{iz} = n_\mathfrak{g} K_{iz}^{(r)}/\nu_{\mathfrak{e}\mathfrak{g}}^{inel,0}.$$

Here, the reference collision frequencies are computed as $\nu_{\mathfrak{e}\mathfrak{h}}^0 = n_\mathfrak{g}^0 \Omega_{\mathfrak{e}\mathfrak{g}}^{(1,0)}(T_\mathfrak{e}^0)$, $\nu_{\mathfrak{e}\mathfrak{e}}^0 = n_\mathfrak{e}^0 \Omega_{\mathfrak{e}\mathfrak{e}}^{(1,0)}(T_\mathfrak{e}^0)$ and $\nu^{inel,0} = n_\mathfrak{g}^0 K_{iz}^{(0)}(T_\mathfrak{e}^0)$ where $n_\mathfrak{g}^0$ is the reference gas density. Note that the inelastic and ionization collisions are normalized to the same reference frequency.

We define the electron-heavy, electron-electron, and inelastic electron-gas Knudsen numbers, and electron-heavy mass ratio, as follows,

$$\mathrm{Kn}_{\mathfrak{e}\mathfrak{h}} = \frac{\sqrt{eT_\mathfrak{e}^0/m_\mathfrak{e}}}{L^0\nu_{\mathfrak{e}\mathfrak{h}}^0}, \quad \mathrm{Kn}_{\mathfrak{e}\mathfrak{e}} = \frac{\sqrt{eT_\mathfrak{e}^0/m_\mathfrak{e}}}{L^0\nu_{\mathfrak{e}\mathfrak{e}}^0}, \quad \mathrm{Kn}_{\mathfrak{e}\mathfrak{g}}^{inel} = \frac{\sqrt{eT_\mathfrak{e}^0/m_\mathfrak{e}}}{L^0\nu_{\mathfrak{e}\mathfrak{g}}^{inel,0}}, \quad \text{and} \quad \varepsilon = \frac{m_\mathfrak{e}}{m_\mathfrak{h}}.$$

The normalized equations read

$$\frac{\partial \hat{n}_{\mathrm{e}}}{\partial \hat{t}} + \frac{\partial}{\partial \hat{x}_i}\hat{n}_{\mathrm{e}}\hat{u}_{\mathrm{e}_i} = \frac{\hat{n}_{\mathrm{e}}\hat{\nu}_{\mathrm{eg}}^{iz}}{\sqrt{\varepsilon}\mathrm{Kn}_{\mathrm{eg}}^{inel}}, \tag{58}$$

$$\frac{\partial}{\partial \hat{t}}\hat{n}_{\mathrm{e}}\hat{u}_{\mathrm{e}_i} + \frac{\partial}{\partial \hat{x}_j}\left(n_{\mathrm{e}}\hat{u}_{\mathrm{e}_i}\hat{u}_{\mathrm{e}_j} + \frac{\hat{p}_{\mathrm{e}}}{\varepsilon}\delta_{ij}\right) = -\frac{\hat{n}_{\mathrm{e}}\hat{E}_i}{\varepsilon} - \frac{1}{\sqrt{\varepsilon}\mathrm{Kn}_{\mathrm{e}\mathfrak{h}}}\sum_{\alpha}^{\mathrm{i,g}}\left(\hat{n}_{\mathrm{e}}\hat{\nu}_{\mathrm{e}\alpha}^{(u,1)}\hat{u}_{\mathrm{e}_i} + \hat{n}_{\mathrm{e}}\hat{\nu}_{\mathrm{e}\alpha}^{(q,1)}\frac{\hat{q}_{\mathrm{e}_i}}{\hat{p}_{\mathrm{e}}}\right), \tag{59}$$

$$\begin{aligned}\frac{3}{2}\frac{\partial \hat{p}_{\mathrm{e}}}{\partial \hat{t}} + \frac{\partial}{\partial \hat{x}_k}\left(\hat{q}_{\mathrm{e}_k} + \frac{3}{2}\hat{p}_{\mathrm{e}}\hat{u}_{\mathrm{e}_k}\right) + \hat{p}_{\mathrm{e}}\frac{\partial \hat{u}_{\mathrm{e}_k}}{\partial \hat{x}_k} = \\ \frac{\sqrt{\varepsilon}}{\mathrm{Kn}_{\mathrm{e}\mathfrak{h}}}\sum_{\alpha}^{\mathrm{i,g}}\left[\hat{n}_{\mathrm{e}}\hat{\nu}_{\mathrm{e}\alpha}^{(T,2)}\left(\hat{T}_\alpha - \hat{T}_{\mathrm{e}}\right) + \hat{n}_{\mathrm{e}}\hat{\nu}_{\mathrm{e}\alpha}^{(u,1)}\hat{u}_{\mathrm{e}}^2 + \hat{n}_{\mathrm{e}}\hat{\nu}_{\mathrm{e}\alpha}^{(q,1)}\frac{\hat{q}_{\mathrm{e}_i}}{\hat{p}_{\mathrm{e}}}\hat{u}_{\mathrm{e}_j}\right] - \frac{1}{\sqrt{\varepsilon}\mathrm{Kn}_{\mathrm{eg}}^{inel}}\sum_{k}^{(excit,iz)}\hat{n}_{\mathrm{e}}\hat{\nu}_{\mathrm{eg}}^{(0,k)}\hat{\phi}_k^*,\end{aligned} \tag{60}$$

$$\begin{aligned}\frac{\partial \hat{q}_{\mathrm{e}_i}}{\partial \hat{t}} + \frac{\partial}{\partial \hat{x}_j}\left(\frac{\hat{r}_{\mathrm{e}_{ij}}}{\varepsilon} + \hat{q}_{\mathrm{e}_i}\hat{u}_{\mathrm{e}_j}\right) + \hat{r}_{\mathrm{e}_{ijk}}\frac{\partial \hat{u}_{\mathrm{e}_k}}{\partial \hat{x}_j} + \hat{q}_{\mathrm{e}_j}\frac{\partial \hat{u}_{\mathrm{e}_i}}{\partial \hat{x}_j} - \frac{5}{2}\frac{\hat{T}_{\mathrm{e}}}{\varepsilon}\frac{\partial \hat{p}_{\mathrm{e}}}{\partial \hat{x}_j}\delta_{ij} = \\ -\frac{1}{\sqrt{\varepsilon}\mathrm{Kn}_{\mathrm{e}\mathfrak{h}}}\sum_{\alpha}^{\mathrm{i,g}}\left[\hat{n}_{\mathrm{e}}\left(\hat{\nu}_{\mathrm{e}\alpha}^{(u,3)} - \frac{5}{2}\hat{\nu}_{\mathrm{e}\alpha}^{(u,1)}\right)\hat{T}_{\mathrm{e}}\hat{u}_{\mathrm{e}_i} + \left(\hat{\nu}_{\mathrm{e}\alpha}^{(q,3)} - \frac{5}{2}\hat{\nu}_{\mathrm{e}\alpha}^{(q,1)}\right)\hat{q}_{\mathrm{e}_i}\right] \\ -\frac{1}{\sqrt{\varepsilon}\mathrm{Kn}_{\mathrm{ee}}}\hat{\nu}_{\mathrm{ee}}^{q}\hat{q}_{\mathrm{e}_i} + \frac{1}{\sqrt{\varepsilon}\mathrm{Kn}_{\mathrm{eg}}^{inel}}\hat{n}_{\mathrm{e}}\hat{u}_{\mathrm{e}_i}\left(\frac{5}{2}\hat{\nu}_{\mathrm{eg}}^{(0,iz)}\hat{T}_{\mathrm{e}} + \sum_{k}^{(excit,iz)}\frac{5}{3}\hat{\nu}_{\mathrm{eg}}^{(0,k)}\hat{\phi}_k^*\right),\end{aligned} \tag{61}$$

$$\begin{aligned}\frac{\partial}{\partial \hat{t}}\hat{p}_{\mathrm{e}_{iijj}} + \frac{\partial}{\partial \hat{x}_k}\left(\hat{r}_{\mathrm{e}_{iijjk}} + \hat{p}_{\mathrm{e}_{iijj}}\hat{u}_{\mathrm{e}_k}\right) + 4\hat{r}_{\mathrm{e}_{ij}}\frac{\partial \hat{u}_{\mathrm{e}_i}}{\partial \hat{x}_j} - 4\frac{\hat{q}_{\mathrm{e}_i}}{\hat{n}_{\mathrm{e}}}\frac{\partial \hat{p}_{\mathrm{e}}}{\partial \hat{x}_j}\delta_{ij} = \\ \frac{\sqrt{\varepsilon}}{\mathrm{Kn}_{\mathrm{e}\mathfrak{h}}}\sum_{\alpha}^{\mathrm{i,g}}\left[\hat{\nu}_{\mathrm{e}\alpha}^{(T,4)}\frac{\hat{p}_{\mathrm{e}}^2}{\hat{n}_{\mathrm{e}}}\left(\frac{\hat{T}_\alpha}{T_{\mathrm{e}}} - 1\right) + 4\hat{n}_{\mathrm{e}}\hat{\nu}_{\mathrm{e}\alpha}^{(u,3)}\hat{T}_{\mathrm{e}}\hat{u}_{\mathrm{e}}^2 - 4\left(\hat{\nu}_{\mathrm{e}\alpha}^{(u,1)} + \hat{\nu}_{\mathrm{e}\alpha}^{(q,3)}\right)\hat{q}_{\mathrm{e}_i}\hat{u}_{\mathrm{e}_i}\right]\end{aligned} \tag{62}$$

$$-\frac{1}{\sqrt{\varepsilon}\mathrm{Kn}_{\mathrm{ee}}}\hat{\nu}_{\mathrm{ee}}^{\Delta}\frac{\hat{p}_{\mathrm{e}}^2}{\hat{n}_{\mathrm{e}}}\Delta_{\mathrm{e}} - \frac{2}{\sqrt{\varepsilon}\mathrm{Kn}_{\mathrm{eg}}^{inel}}\sum_{k}^{(excit,iz)}\left(\frac{\hat{p}_{\mathrm{e}}^2}{\hat{n}_{\mathrm{e}}}\right)\left(2\hat{\nu}_{\mathrm{eg}}^{(1,k)}\hat{\phi}_k^* - \hat{\nu}_{\mathrm{eg}}^{(0,k)}\hat{\phi}_k^{*^2}\right). \tag{63}$$

B. Generalized Chapman-Enskog expansion

As explained by Struchtrup & Torrilhon[30], a regularization of the moment model can be obtained by expanding the macroscopic variables in series of the Knudsen number. In this work, we exploit the smallness of the electron to heavy mass ratio as well as the fact that in weakly-ionized plasmas, the Knudsen number of the electron-gas collisions is smaller than the electron-electron collision Knudsen number and the latter is smaller than the inelastic electron-gas collisions, as follows,

$$\mathrm{Kn}_{\mathrm{e}\mathfrak{h}} = \mathscr{O}\left(\varepsilon^{1/2}\right) \lesssim \mathrm{Kn}_{\mathrm{ee}} \ll \mathrm{Kn}_{\mathrm{eg}}^{inel}. \tag{64}$$

With this ordering, one can see that the non-dimensional equations of the odd moments follow a different structure than the even moments. The momentum and heat-flux equations contain terms

in the fluxes that are of the same order of magnitude of the elastic collisional terms, i.e., of order $\mathscr{O}(\varepsilon^{-1})$. Alternatively, the relaxation terms of the elastic collisions are multiplied by the mass ratio in the energy and the fourth moment equations and hence the elastic collisional terms are of the same order as the flux terms, i.e., of order $\mathscr{O}(\varepsilon^{0})$. This is consistent with the two-term approximation that assumes that the anisotropic part of the distribution function is much smaller than the isotropic one due to the effect of the electron-gas collisions.

As a result, we can obtain the velocity and heat flux from the terms of order $\mathscr{O}(\varepsilon^{-1})$ of the equations, that in dimensional form read

$$\nabla p_{\mathfrak{e}} = -e n_{\mathfrak{e}} \boldsymbol{E} - m_{\mathfrak{e}} n_{\mathfrak{e}} \nu_{\mathfrak{eh}}^{(u,1)} \boldsymbol{u}_{\mathfrak{e}} - m_{\mathfrak{e}} n_{\mathfrak{e}} \nu_{\mathfrak{eh}}^{(q,1)} \frac{\boldsymbol{q}_{\mathfrak{e}}}{p_{\mathfrak{e}}}, \tag{65}$$

$$\frac{5}{2}(1+2\Delta_{\mathfrak{e}})\frac{e p_{\mathfrak{e}}}{m_{\mathfrak{e}}}\nabla T_{\mathfrak{e}} + \frac{5}{2}\frac{(eT_{\mathfrak{e}})^2}{m_{\mathfrak{e}}}\left(\Delta_{\mathfrak{e}}\nabla n_{\mathfrak{e}} + n_{\mathfrak{e}}\nabla\Delta_{\mathfrak{e}}\right) = -p_{\mathfrak{e}}\left(\nu_{\mathfrak{eh}}^{(u,3)} - \frac{5}{2}\nu_{\mathfrak{eh}}^{(u,1)}\right)\boldsymbol{u}_{\mathfrak{e}} - \left(\nu_{\mathfrak{eh}}^{(q,3)} + \nu_{\mathfrak{ee}}^{q} - \frac{5}{2}\nu_{\mathfrak{eh}}^{(q,1)}\right)\boldsymbol{q}_{\mathfrak{e}}. \tag{66}$$

These equations form a system of Stefan-Maxwell equations where the fluxes $n_{\mathfrak{e}}\boldsymbol{u}_{\mathfrak{e}}$ and $\boldsymbol{q}_{\mathfrak{e}}$ can be expressed as a function of the collisional frequencies, the temperature, the density, the contracted fourth moment, and the spatial gradients of these variables, as follows,

$$\boldsymbol{u}_{\mathfrak{e}} = -D_{\mathfrak{e}}\left(\frac{1}{n_{\mathfrak{e}}}\nabla n_{\mathfrak{e}} + (1+\chi_{\mathfrak{e}})\nabla\ln T_{\mathfrak{e}} + \alpha_{\mathfrak{e}}\nabla\Delta_{\mathfrak{e}}\right) - \mu_{\mathfrak{e}}\boldsymbol{E}, \tag{67}$$

$$\boldsymbol{q}_{\mathfrak{e}} = \Lambda_{\mathfrak{e}} n_{\mathfrak{e}}\boldsymbol{u}_{\mathfrak{e}} - \kappa_{\mathfrak{e}}\nabla T_{\mathfrak{e}} - \vartheta_{\mathfrak{e}}\nabla n_{\mathfrak{e}} - \varkappa_{\mathfrak{e}}\nabla\Delta_{\mathfrak{e}}. \tag{68}$$

The resulting transport coefficients are functions of the EEDF that is parametrized by the density, the temperature, and the fourth-order moment $\Delta_{\mathfrak{e}}$ and the integrals of the collisional cross-sections. We show the analytical expressions of the transport coefficients in Appendix B.

We show in Eq. (67) that our model captures the classical Fick's diffusion (diffusion of particles produced by density gradients), thermophoresis (diffusion produced by temperature gradients) and the electric mobility. In addition, our model captures a novel effect that produces diffusion of particles due to spatial gradients of the normalized fourth moment. This represents transport processes due to spatial variations in the shape of the EEDF. This transport effect can be seen as a non-local effect when the EEDF is not Maxwellian and is fundamental in order to regularize the equation for the contracted fourth-order moment, as it will be shown in the following section. Analogously, the heat flux Eq. (68) has contributions due to the convection (proportional to the particle flux), thermal conduction (proportional to temperature gradients), the Dufour effect (proportional to density gradients). As in the particle flux, there is a non-local effect due to spatial gradients of the contracted fourth moment.

C. Regularized equations

The system of regularized moment equations at order $\mathscr{O}(\varepsilon^0)$ corresponds to the conservation laws of particle density, electron energy, and contracted fourth moment. For convenience, the dimensional equations can be written in conservation form, as follows,

$$\frac{\partial n_{\mathfrak{e}}}{\partial t}+\frac{\partial}{\partial x_k}n_{\mathfrak{e}}u_{\mathfrak{e}_k}=n_{\mathfrak{e}}n_{\mathfrak{g}}K_{iz}^{(0)}, \tag{69}$$

$$\frac{3}{2}\frac{\partial p_{\mathfrak{e}}}{\partial t}+\frac{\partial}{\partial x_k}\left(\frac{5}{2}p_{\mathfrak{e}}u_{\mathfrak{e}_k}+q_{\mathfrak{e}_k}\right)=-en_{\mathfrak{e}}u_{\mathfrak{e}_k}E_k+\sum_{\alpha}^{\mathfrak{i},\mathfrak{g}}\frac{m_{\mathfrak{e}}}{m_\alpha}n_{\mathfrak{e}}\nu_{\mathfrak{e}\alpha}^{(T,2)}e\left(T_\alpha-T_{\mathfrak{e}}\right)-\sum_{k}^{(excit,iz)}n_{\mathfrak{e}}\nu_{\mathfrak{e}\mathfrak{g}}^{(0,k)}e\phi_k^*, \tag{70}$$

$$\begin{aligned}\frac{\partial p_{\mathfrak{e}_{iijj}}}{\partial t}+\frac{\partial}{\partial x_k}\left(\frac{7}{3}p_{\mathfrak{e}_{iijj}}u_{\mathfrak{e}_k}+14\frac{p_{\mathfrak{e}}}{\rho_{\mathfrak{e}}}q_{\mathfrak{e}_k}\right)&=-4\frac{e}{m_{\mathfrak{e}}}q_{\mathfrak{e}_k}E_k-10\frac{e}{m_{\mathfrak{e}}}p_{\mathfrak{e}}u_{\mathfrak{e}_k}E_k+\sum_{\alpha}^{\mathfrak{i},\mathfrak{g}}\frac{m_{\mathfrak{e}}}{m_\alpha}\nu_{\mathfrak{e}\alpha}^{(T,4)}\frac{p_{\mathfrak{e}}^2}{\rho_{\mathfrak{e}}}\left(\frac{T_\alpha}{T_{\mathfrak{e}}}-1\right)\\&-\frac{p_{\mathfrak{e}}^2}{\rho_{\mathfrak{e}}}\nu_{\mathfrak{e}\mathfrak{e}}^{\Delta}\Delta_{\mathfrak{e}}-4\nu_{\mathfrak{e}\mathfrak{e}}^{q}q_{\mathfrak{e}_k}u_{\mathfrak{e}_k}-2n_{\mathfrak{g}}\left(\frac{p_{\mathfrak{e}}^2}{\rho_{\mathfrak{e}}}\right)\sum_{k}^{(excit,iz)}\left(2K_k^{(1)}\left(\frac{\phi_k^*}{T_e}\right)-K_k^{(0)}\left(\frac{\phi_k^*}{T_e}\right)^2\right).\end{aligned} \tag{71}$$

Here, the closure of the system of equations uses the velocity and heat flux of Eqs. (65) and (66). Note that we have neglected the term that is proportional to $m_{\mathfrak{e}}/m_{\mathfrak{g}}\Delta_{\mathfrak{e}}T_{\mathfrak{g}}$ that appears in Eq. (39).

The first advantage of the regularized equations as compared to Grad's equations is the reduced number of variables to be computed, as the velocity and heat flux are computed as transport fluxes through an algebraic equation. However, the most important difference is related to the mathematical structure of Eqs. (69)-(71), which differs greatly from the Grad's system of equations. Instead of a hyperbolic system (i.e., fluxes that depend as $F(\mathbf{U})$), the system contains also parabolic terms (i.e., fluxes that depend as $F(\mathbf{U},\nabla\mathbf{U})$). In this sense, we note the importance of the terms that are proportional to $\nabla\Delta_{\mathfrak{e}}$ in the particle and heat transport fluxes expressions.

In order to illustrate the mathematical structure of the regularized fourth-moment balance equation, we consider the fourth-moment balance Eq. (71) under the effect of a constant electric field without density nor temperature gradients. By injecting Eqs. (65) and (66), and the definition of normalized fourth moment, Eq. (25), into Eq. (71) the equation for the normalized fourth moment reads the following familiar form

$$\frac{\partial\Delta_{\mathfrak{e}}}{\partial t}-\nabla\cdot\left(D_\Delta\nabla\Delta_{\mathfrak{e}}+\mu_\Delta\mathbf{E}\Delta_{\mathfrak{e}}\right)=\sigma_\Delta E^2-P_{loss}^{(\Delta)}-\frac{2}{15}\nu_{\mathfrak{e}\mathfrak{e}}^{\Delta}\Delta_{\mathfrak{e}}, \tag{72}$$

where D_Δ, μ_Δ, and σ_Δ are positive coefficients that are given in Appendix B, and $P_{loss}^{(\Delta)}$ groups the loss terms due to electron-heavy elastic and inelastic collisions. Indeed, Eq. (72) is an advection-diffusion-reaction equation for the scalar normalized fourth moment $\Delta_{\mathfrak{e}}$. The diffusion is produced

by electron-electron and electron-heavy elastic collisions and gradients in Δ_e whereas the electric field is responsible for the advection. As in the energy equation, the equation for the fourth-order moment has a production term that is proportional to the square of the electric field and a loss term produced by the collisions with the other species. Finally, the last term represents the relaxation to a Maxwellian at the scales of the electron-electron collisional time. We recall that negative values of Δ_e represent Druyvestein-like distribution. Thus, the collisions with the gas tend to deplete the distribution function. Alternatively, oscillating or DC electric fields have the opposite effect, as well as the electron-electron elastic collisions.

VI. SPATIALLY HOMOGENEOUS RESULTS

In this work, we validate the collision production terms and the transport coefficients through the comparison of the moment model with spatially homogeneous solutions to kinetic simulations. We will consider the cross-sections of argon[52] for both the kinetic and the moment model. The equations for each validation case are presented in the Appendix C.

A. Relaxation to a Maxwellian

We first study the effect of the electron-electron collisions standalone. For this, we study a relaxation to thermal equilibrium from a non-equilibrium state. This is a fundamental property that needs to be fulfilled by any moment model. In this first case, we solve for the spatially homogeneous fourth-moment equation, Eq. (C1), with a fourth-order Runge-Kutta scheme. We initialize the equation in thermal non-equilibrium, with a perturbation in the normalized fourth moment, as follows, $\Delta_e(t=0) = -0.1$. The density and temperature remain constant at $n_e = 10^{17}$ m^{-3} and $T_e = 5$ eV, without perturbations in the anisotropic part of the distribution function.

We compare the moment simulation to a DSMC model that discretizes the Landau collision operator with the Nanbu-Babovsky scheme as proposed by Dimarco et al.[53] To initialize the kinetic simulation, we sample the particles following the non-equilibrium distribution function of Eq. (28) with the above-mentioned perturbations in the fourth moment. The DSMC results use 1000 particles. The results present the 95% confidence interval of 25 statistically independent simulations of the same relaxation.

In Fig. 4, we show the comparison between the moment model and the DSMC of the evolution

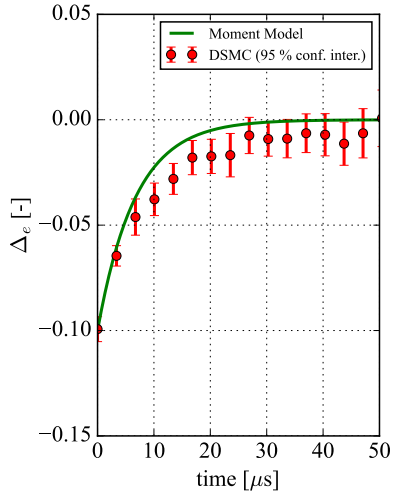

FIG. 4. Relaxation to thermal equilibrium from a non-Maxwellian function due to electron-electron collisions, with a DSMC model and a 9-M Grad model.

contracted fourth moment. In the case of the kinetic simulations, we compute the fourth moment of the particle distribution and present the error bars that correspond to the 95% confidence interval corresponding to the ensemble of realizations. Both simulations relax to a Maxwellian distribution function ($\Delta_e = 0$). The relaxation time is similar to the DSMC simulation with a discretized Landau-Fokker-Planck operator for Coulomb collisions. Finally, note that, as the electron-electron collisional frequencies of Eq. (55) are positive for all electron temperatures and hence the system relaxed to thermal equilibrium.

B. Collisional cooling of electrons in a gas

In the second case, we study the cooling of electrons due to collisions with an argon gas at room temperature ($T_g = 300$ K). As the simulation has no electric field nor spatial gradients, only the isotropic part of the electron distribution function evolves in time. The main energy loss mechanism is due to inelastic collisions with the gas. However, only electrons with energies above the excitation and ionization potential lose the energy, resulting in a depopulation of the EEDF at high energies. As a result, a fluid model with a Maxwellian EEDF is not able to properly predict the cooling rate as it overestimates the population of electrons at high energies.

In this simulation, we consider electron-electron elastic, electron-argon elastic, and inelastic collisions. The ionization collision is treated as an inelastic collision and hence the electron den-

sity does not grow during the simulation. The moment model considers the evolution equations of the electron temperature and contracted fourth moment, i.e., Eqs. (C2) and (C3). We compare this model to a fluid model that considers a Maxwellian distribution function and solves only for the temperature equation, i.e., Eq. (C2) with the collisional rates computed with a Maxwellian distribution function. The DSMC simulation discretizes the electron-electron collisions as discussed in the previous case and the electron-argon collisions with a null-collision method[54]. We initialize the simulations with a Maxwellian distribution function, i.e., $\Delta_e = 0$, at $T_e = 5$ eV and an electron density of $n_e = 10^{17}$ m^{-3} that remains constant. We consider two ionization degrees of $n_e/n_g = 10^{-2}$ and 10^{-3} with the argon gas at $T_g = 300$ K that remains constant.

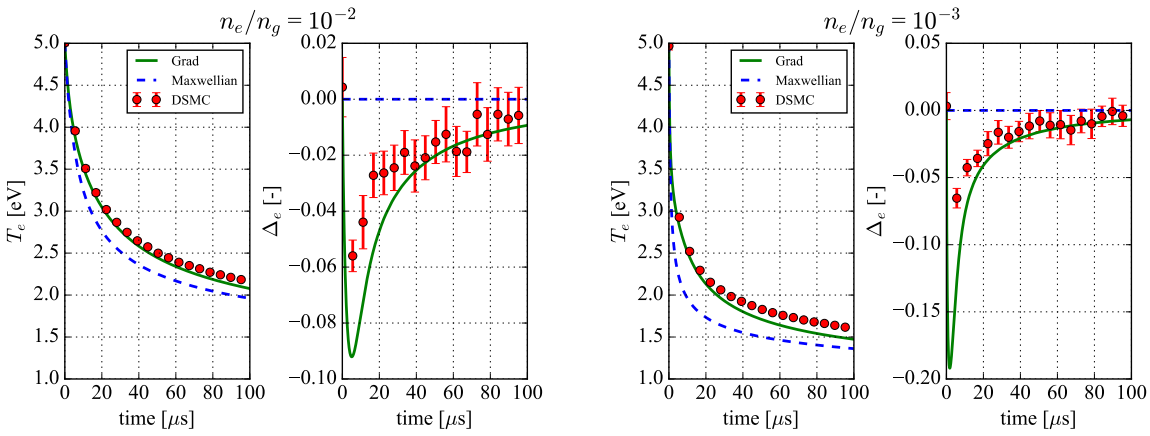

FIG. 5. Evolution of the temperature and the fourth moment of electrons colliding with an argon gas at two different ionization degrees (10^{-2} on the left and 10^{-3} on the right). We show the comparison between DSMC, the moment model (Grad) and the model with a Maxwellian dirstribution.

The evolution of the temperature and contracted fourth moment is presented in Fig. 5 for both considered ionization degrees. As expected, the fluid model with a Maxwellian EEDF predicts a much faster relaxation, particularly in the case with lower ionization degree. For instance, for $n_e/n_g = 10^{-2}$, the fluid model with a Maxwellian EEDF cools down to 2.5 eV in approximately 30 μs, whereas the moment method and the DSMC reach this temperature around 20 μs later. Similarly, for $n_e/n_g = 10^{-3}$, the fluid model with a Maxwellian cools down to 2 eV in around 10 μs whereas the kinetic and higher-order moment simulations reach this temperature in more than twice this time.

In Figs. 6 and 7, we present the evolution of the EEDF with ionization degrees of $n_e/n_g = 10^{-2}$ and $n_e/n_g = 10^{-3}$, respectively. As expected, the EEDF of the DSMC simulation depopulates

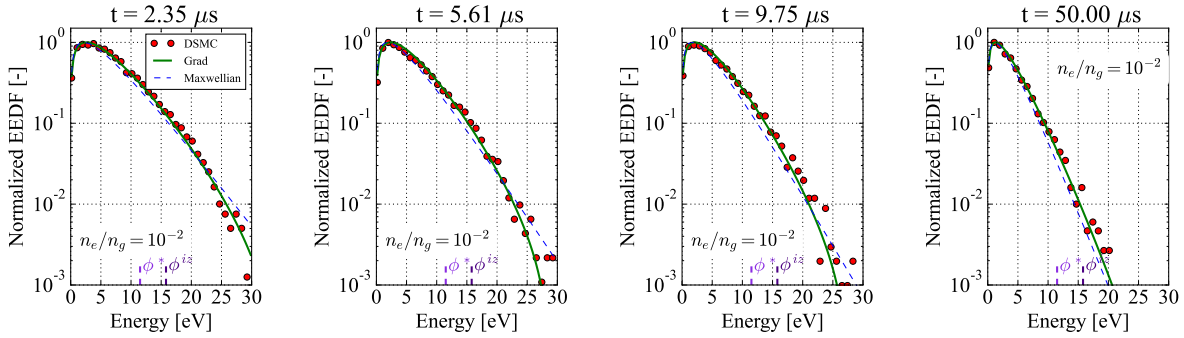

FIG. 6. Simulation of electron cooling by collisions with a gas at an ionization degree of $n_e/n_g = 10^{-2}$: Comparison of the EEDF as computed by DSMC, a moment model considering the energy and fourth moment equations (Grad), and a model considering only the energy equation (Maxwellian). The excitation and ionization energies are marked in purple.

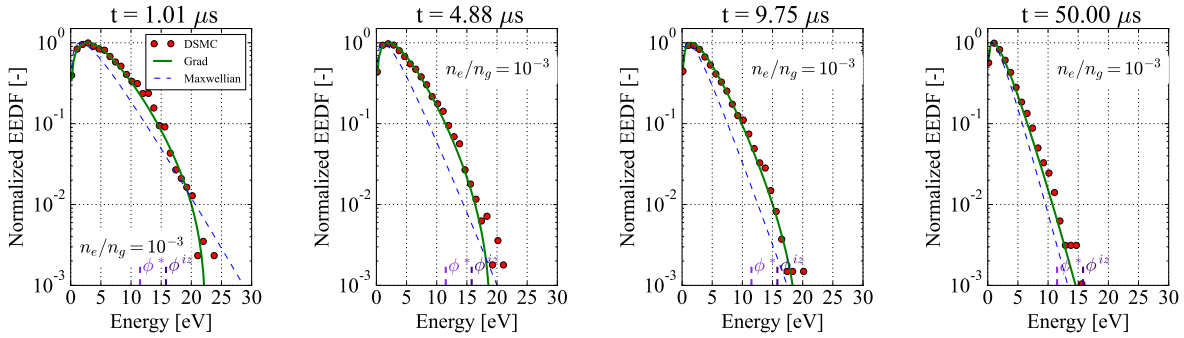

FIG. 7. Simulation of electron cooling by collisions with a gas at an ionization degree of $n_e/n_g = 10^{-3}$: Comparison of the EEDF as computed by DSMC, moment model considering the energy and fourth moment equations (Grad), and a model considering only the energy equation (Maxwellian). The excitation and ionization energies are marked in purple.

faster at energies that are larger than the excitation and ionization potential (marked with purple lines in the figures). For $n_e/n_g = 10^{-3}$, this depopulation occurs faster as the collision frequency is proportional to the gas density. After the first instants of the simulation, the EEDF Maxwellizes by electron-electron collisions, which frequency is larger for lower electron temperatures. In the high-order moment model, the depopulation at high energies is self-consistently captured for negative values of Δ_e. Moreover, we realize that the EEDF of the moment model is quantitatively very similar to the DSMC result. As a result, as the inelastic collision rates depend on the contracted

fourth moment (cf., Eq. (49)), the energy losses are better captured than in the case of a fluid model that considers a Maxwellian distribution. In addition, as compared to the DSMC model, the moment model is computationally very efficient as it solves only for two equations and the collision rates can be pre-computed and saved into lookup tables as a function of T_e and Δ_e.

C. Comparison to a two-term Boltzmann solver

We study the regularized moment equations that were presented in Section V. We compare the moment model to the solutions of the Boltzmann solver in the two-term approximation BOLSIG+[4,55]. In addition, we compare the solutions to a fluid model that uses the collisional terms with a BGK operator with the frequency computed as a rate with a Maxwellian distribution function. This model is often used in fluid models for low-temperature plasmas at low pressure, e.g., refs.[18–20,56]. In a first step, we neglect the electron-ion collisions in order to verify separately the different contributions due to the different species. No growth of the electron density is included in the model and the ionization collision is treated as an excitation collision.

We study spatially homogeneous solutions with an external DC electric field. The high-order moment system of equations solves for a balance equation of the temperature Eq. (C4) and the contracted fourth moment Eq. (C5), while the drift velocity and the heat flux are computed as a function of the electric field and the transport coefficients, as defined in Eqs. (B3)-(B4). As explained by Hagelaar[55], the solution depends on the reduced electric E/n_g, the ionization degree n_e/n_g, and the electron density that in all the cases is set to $n_e = 10^{17}$ m^{-3}.

For each value of electric field and ionization degree we solve the system of equations until convergence to a steady state. We use a Runge-Kutta fourth-order scheme for the discretization of the equations, and implicit backward differentiation formula (BDF) for the stiffer cases.

In Fig. 8, we show the comparison of the electron energy probability functions as computed by the Boltzmann solver, the moment model, and the model with a Maxwellian distribution. We show the solution for $n_e/n_g = 10^{-2}$ and 10^{-3}, with reduced electric fields between 1 Td and 50 Td. As in the previous test cases, the solution of the energy distribution functions of the 9-M Grad model self-consistently captures the slope of the distribution function at low energies as well as the depopulation at high energies. At low values of the electric field the EEPF seems to be closer to a Maxwellian in the moment model. This can be explained due to a difference in the model of the electron-electron collision frequency that is slightly higher in the case of a

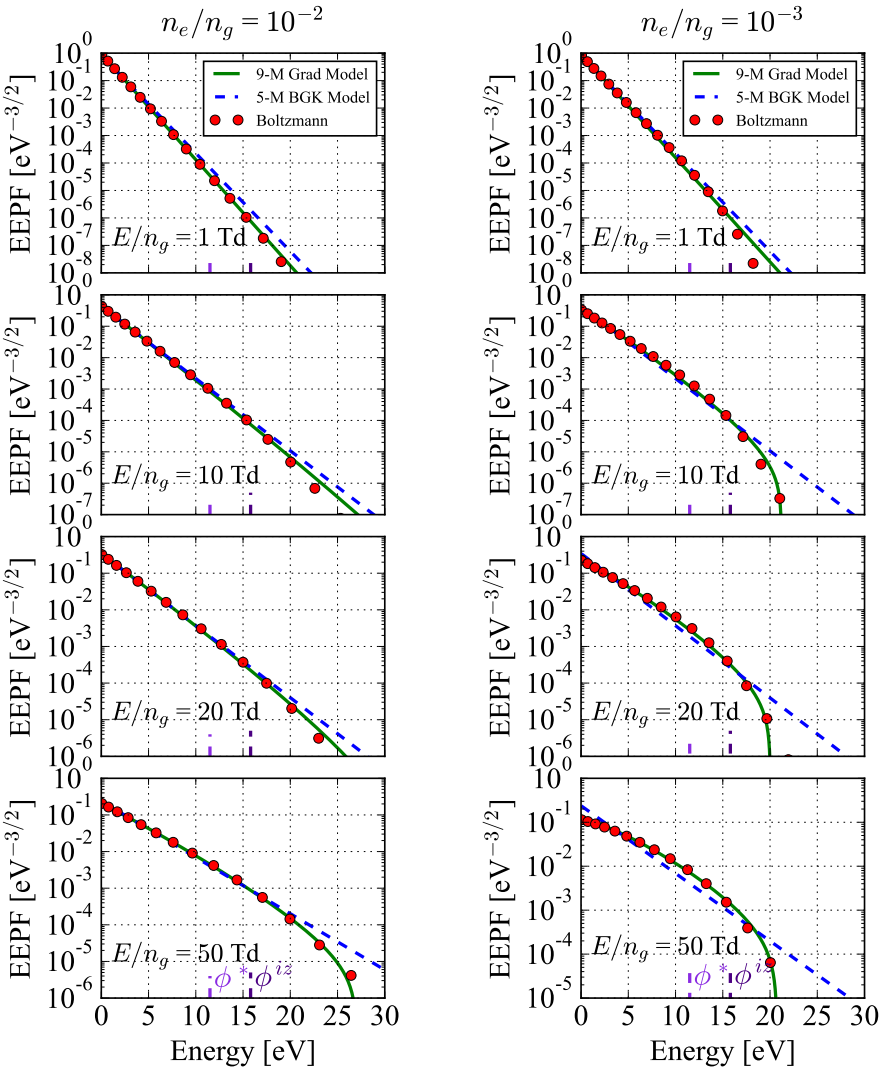

FIG. 8. Comparison of the computed EEPF between Boltzmann solver, Grad 9-M model and a 5-M model with a BGK operator for two ionization degrees, $n_e/n_g = 10^{-2}$ and 10^{-3} and reduced electric fields between 1 Td and 50 Td. The Grad moment model captures the slope of the distribution function at low energies as well as the depopulation at high energies as computed by the Boltzmann solver. The main differences are found at energies above the excitation potential.

Boltzmann operator. Nevertheless, the moment model finds a very good agreement with the two-term Boltzmann solution.

In Fig. 9, we show the evolution of the macroscopic variables for $E/n_{\mathfrak{g}} = 50$ Td and $n_{\mathfrak{e}}/n_{\mathfrak{g}} = 10^{-3}$. As it can be seen, the electric field produces a drift velocity, which increases the electron

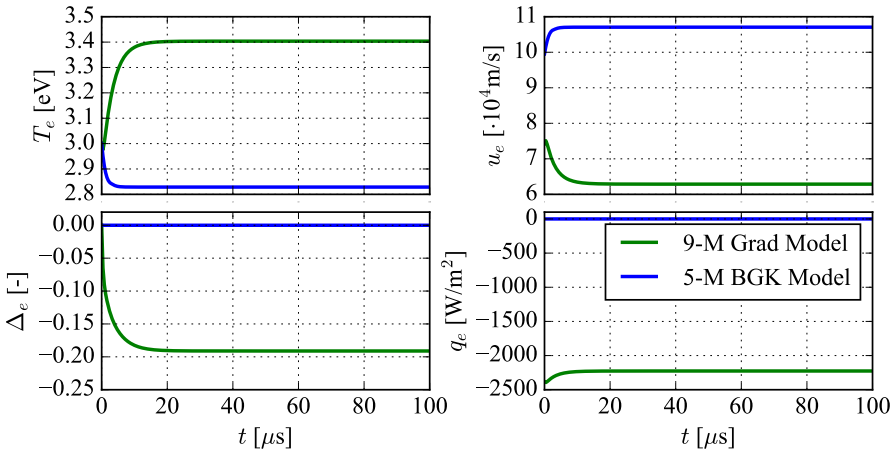

FIG. 9. Comparison of the evolution of the fluid variables for 5-M BGK solver and 9-M Grad model at $E/N = 50$ Td and $n_\mathfrak{e}/n_\mathfrak{g} = 10^{-3}$.

temperature by Joule heating through electron-gas elastic collisions. Similarly, this electric field produces a heat-flux in the opposite direction. The temperature converges to an equilibrium between the Joule heating and the losses from inelastic and elastic collisions (which strongly depend on the fourth moment). In addition, the converged fourth moment is the result of a similar equilibrium. The losses of fourth moment are produced by elastic and inelastic collisions with the gas and the thermal friction. This losses are balanced by the Maxwellization due to electron-electron collisions, and the gain of fourth moment due to the drift and heat flux (proportional to $u_\mathfrak{e}^2$ and $q_\mathfrak{e}^2$). In Fig. 9, we can see that the electron temperature is higher in the case of the moment model even though the drift velocity is smaller. This is explained by the fact that, as $\Delta_\mathfrak{e} = -0.2$, the distribution function is depleted at high energies and hence the energy losses are much smaller than in the Maxwellian case for the same temperature. Note that the values of $\Delta_\mathfrak{e}$ and $T_\mathfrak{e}$ are similar to these shown in the experimental results of Fig. 2.

We compute the mean energy, ionization and excitation rates, reduced mobility, diffusion coefficient, and reduced energy mobility as a function of the electric field, as defined in Appendix B. Note that, as opposed to the Boltzmann solver, the transport coefficients are not computed with the EEDF, but directly from the definitions of Eqs. (B1)-(B7). In Fig. 10, we present the electron properties computed for 41 values of the reduced electric field between 10^{-1} Td and 10^3 Td and $n_\mathfrak{e}/n_\mathfrak{g} = 10^{-2}$. In this range of electric fields, the transport coefficients and rates are quantitatively very similar to those computed with the two-term Boltzmann simulation. In particular, the

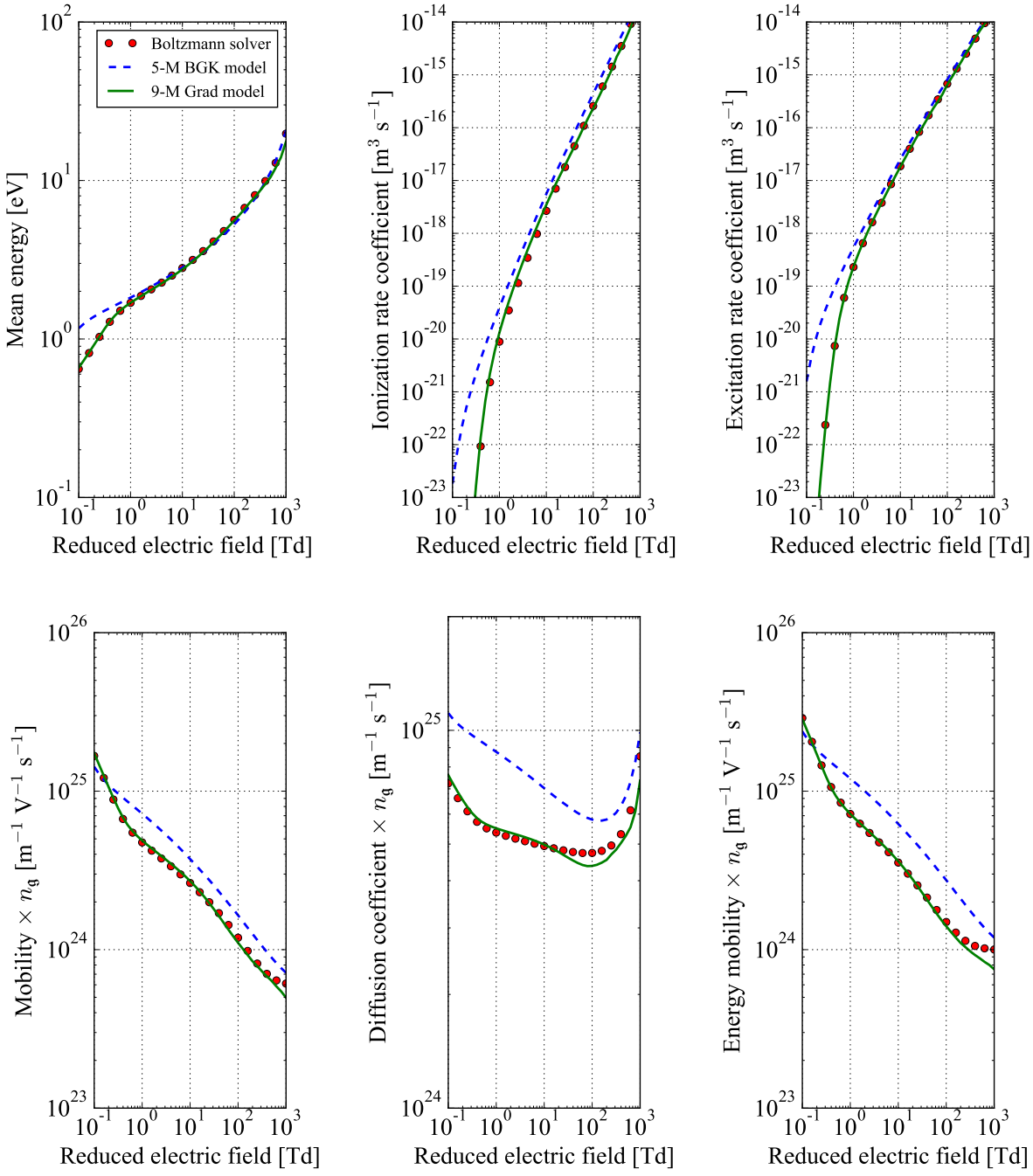

FIG. 10. Mean energy, ionization and excitation rate coefficients, reduced mobility, reduced diffusion coefficient, and reduced energy mobility, as a function of the reduced electric field for an argon plasma, considering electron-gas and electron-electron collisions. We compare the solution of a Boltzmann solver (red circles), a 5-M model with a BGK collision operator (blue), and the 9-M Grad model (green).

high-order moment model captures the ionization and excitation rates that are orders of magni-

tude different from the BGK model and that are much closer to these computed by the Boltzmann solver (with a difference below 10%). Similarly, the rest of transport coefficients of the high-order moment present a remarkable improvement as compared to the BGK model when they are compared to the Boltzmann solver. The high-order moment model has the largest errors at high electric fields, where the anisotropic part of the distribution function is no longer small and higher-order moments in the anisotropic part of the distribution function are needed.

In Fig. 11, we study the dependence of the transport coefficients and rates on the ionization degree. To compute these properties, we carry out 31 simulations with different ionization degrees for each value of electric field. In a classical fluid model that considers a Maxwellian distribution function (5-M model), the electron temperature balance is independent of the ionization degree (see Eq. (C7)). This is due to the fact that the collisional frequencies only depend on the electron temperature and gas density and therefore the balance equation for the temperature in 0D does not depend on the electron density. However, in the high-order moment model, the mobility, energy mobility, and the balance equation of the fourth moment depend as well on the electron-electron collision frequency and hence on the ionization degree. In Fig. 11, we study four values of reduced electric field, between 1 and 500 Td. We show that the dependence on the ionization degree is well captured by the high-order moment model. The main difference is found in the ionization rate at low electric field. This can be explained by an overestimation of the electron-electron collision rate at low temperatures that produces a distribution function that is more Maxwellian than the Boltzmann solver. Similarly, differences in the computation of the diffusion coefficient are found. Even though the results of the 9-M Grad model largely improve those of the 5-M BGK model with a BGK operator, the Grad model finds larger disagreement with the kinetic solution for increasing values of electric field and decreasing ionization degrees. This is due to two reasons. First, the non-equilibrium conditions are stronger at lower ionization degrees because of the effect of the collisions with the gas at low temperature. Second, in the presence of higher electric fields, the non-equilibrium conditions are also strong due to the large drift between the electrons and the gas. Note that although the mean energy as computed by the 5-M BGK is in better agreement with the kinetic solution at 500 Td, the rest of properties are overestimated by the 5-M BGK model. For this reason, even though the 5-M overestimates the energy losses (due to a larger inelastic and ionization rates), more power is absorbed (due to a larger mobility) resulting in the correct mean energy. However, as the transport and collision rate coefficients are overestimated, we expect that the 5-M BGK model would not be able to correctly predict the plasma conditions

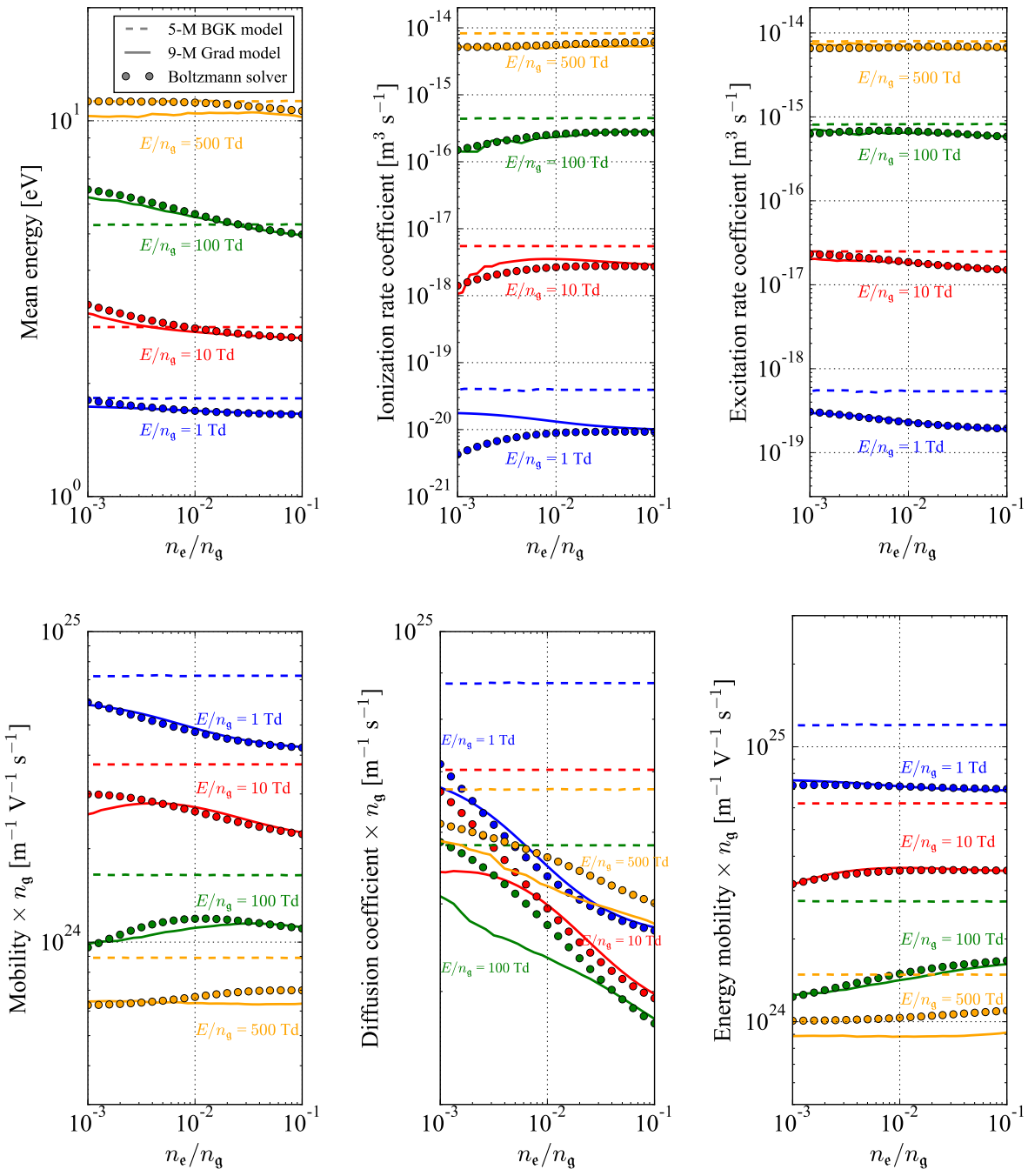

FIG. 11. Comparison of the electron transport coefficients of an argon plasma are computed with a Boltzmann solver and the high-order moment model for different ionization degrees.

in a multi-dimensional simulation considering self-consistent ionization.

Finally, we study the effect of the electron-ion collisions. We recall that we use a Boltzmann operator with a Coulomb potential cut-off at the Debye length, which is different from the model

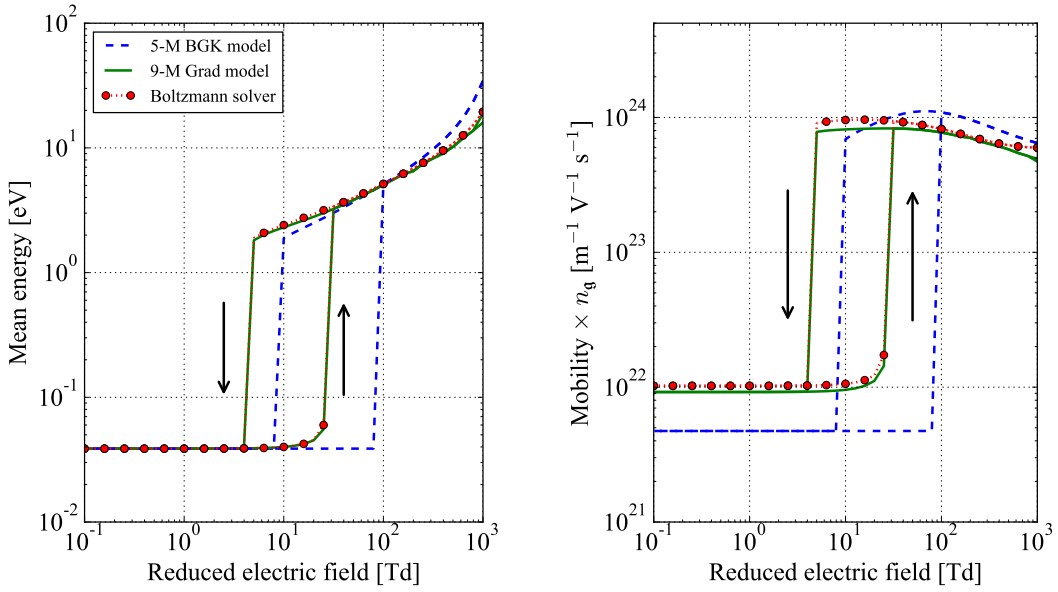

FIG. 12. Effect of the electron-ion collisions on the mean energy and reduced mobility as a function of the reduced electric field at $n_e/n_g = 10^{-2}$. The moment model also presents a bistability and hysteresis at the same critical values of electric field as found by the Boltzmann solver whereas the 5-M BGK model is not able to correctly predict the critical electric field.

in the two-term Boltzmann solver. Both in the moment model and in the Boltzmann solver, we assume the ions to be in thermal equilibrium with the gas and to have the same density of the electrons. As discussed by Hagelaar[4], when the electron-ion collisions are included in the model, an abrupt change in electron mobility and electron mean energy appears above a certain critical electric field. Below this critical value, the electrons are in thermal equilibrium with the ions, and above this values the electrons establish an equilibrium with the neutral gas. In Fig. 12, we present the computed mean energy and reduced mobility including electron-ion collisions. The bistability is also present in the high-order moment model. We note that the critical electric field is the same for both models. In addition, the same hysteresis is present in the moment model, predicting similar values for the critical electric field. On the other hand, the 5-M model that uses collision frequencies as usually used in simplified plasma models, is not able to correctly predict the critical values of the electric field in the bistability.

VII. CONCLUSIONS

The goal of this work is the development of a moment model to describe electron transport phenomena with non-Maxwellian EEDF in partially-ionized plasmas at low pressure. The characterization of the electron energy distribution function is fundamental to describe plasma discharges as the ionization, inelastic rates and electron transport coefficients are a function of the EEDF. The model self-consistently captures non-Maxwellian EEDFs through the resolution of scalar and vectorial moments up to the contracted fourth moment whereas the collisional terms of the equations are consistently derived from the kinetic equation.

We have derived the moment evolution equations with Grad's method. The moments of the multi-species collisional operator have been consistently derived, including electron-electron and electron-heavy (neutrals and ions) elastic collisions as well as inelastic and ionization collisions. The set of equations includes effects that are usually neglected in simplified fluid models for partially-ionized plasmas such as the thermal friction or the effect of the EEDF in the inelastic collision rates and the electron-gas energy relaxation frequency. Note that the latter can have an impact in the quantification of the gas heating term.

We have regularized the Grad's moment equations, based on a Chapman-Enskog expansion that exploits the electron-heavy mass ratio and the ionization degree. The resulting regularized moment equations are a system of mixed hyperbolic-parabolic-reaction equations for the scalar even moments whereas the vectorial moments are computed from a system of Stefan-Maxwell equations. The transport equation for the fourth-moment has a mathematical structure that is similar to the energy equation, including an advection and diffusion terms, a gain due to the electric field and losses due to elastic and inelastic collisions with the gas. In the transport fluxes of particles and energy, in addition to Fick's diffusion, thermodiffusion and heat conduction, a novel non-local effect appears due to the spatial variation of the EEDF when it is not Maxwellian.

Numerical solutions of the moment system under spatially-homogeneous conditions are compared to kinetic simulations. The model proves to relax to thermodynamic equilibrium due to electron-electron collisions. In addition, the depletion of the EEDF at high energies due to electron-gas inelastic collisions is correctly captured by the moment model, which has a large impact in the estimation of the cooling rate of electrons in partially-ionized plasmas. Finally, we compare to a two-term Boltzmann solver under the presence of an electric field. The EEDF and the transport coefficients as computed by the moment model are quantitatively very close to those

found by kinetic simulations. In addition, the numerical experiments show the great improvement as compared to a BGK operator.

We have studied conditions that are representative of high plasma density discharges at low pressure. These conditions are characteristic of ICP discharges at low pressure (< 50 mTorr) with plasma densities of $10^{16} \lesssim n_e \lesssim 10^{19}$ m^{-3}, such as those presented in Fig. 2 from Aneslaand et al[46]. Other plasmas such as capacitively coupled or atmospheric pressure dicharges present stronger non-equilibrium conditions, due to higher gas pressures or lower ionization degrees. Under stronger non-equilibrium conditions, the methodology that has been presented, including the choice of moments, determination of the collisional terms and the regularization of the equations, can be extended. This can be of particular interest in the transition from streamer to arc. Under stronger non-equilibruim conditions, a possible extension is to consider higher-order moments in order to capture larger perturbations in the EEDF, consequence of higher gas pressures, or other anisotropies, e.g., pressure tensor, more adapted for the presence of a magnetic field. Numerical solutions of the set of regularized equations in 1D will be explored in future work as well as a comparison to experimental results of an ICP discharge.

ACKNOWLEDGEMENTS

The authors would like to thank Prof. Jean-Luc Raimbault for having carefully read the manuscript and for helpful discussions. B. Esteves acknowledges the financial support from L' Agence Innovation Défense de la Délégation Générale de L'Armement (DGA) and École Polytechnique.

Appendix A: Integrals over the scattering angles of the collision and change of reference frame

1. Expressions for the integration over the scattering angles

The integral over the scattering angles in an electron-heavy elastic collision reads

$$\mathscr{F}^{el}_{\mathfrak{e}\alpha}(\boldsymbol{g},\boldsymbol{G}) = \begin{pmatrix} 0 \\ g_i Q^{(1)}_{\mathfrak{e}\alpha} \\ (g_j G_j) Q^{(1)}_{\mathfrak{e}\alpha} \\ \frac{1}{2}\left[2(g_j G_j)G_i + G^2 g_i + \left(\frac{\mu_{\mathfrak{e}\alpha}}{m_{\mathfrak{e}}}\right)^2 g^2 g_i\right] Q^{(1)}_{\mathfrak{e}\alpha} - \frac{1}{2}\left(\frac{\mu_{\mathfrak{e}\alpha}}{m_{\mathfrak{e}}}\right)\left[g^2 G_i - 3(G_j g_j) g_i\right] Q^{(2)}_{\mathfrak{e}\alpha} \\ 2\left[G^2 + \left(\frac{\mu_{\mathfrak{e}\alpha}}{m_{\mathfrak{e}}}\right)^2 g^2\right](G_j g_j) Q^{(1)}_{\mathfrak{e}\alpha} - \left(\frac{\mu_{\mathfrak{e}\alpha}}{m_{\mathfrak{e}}}\right)\left[g^2 G^2 - 3\left(G_j g_j\right)^2\right] Q^{(2)}_{\mathfrak{e}\alpha} \end{pmatrix}. \tag{A1}$$

Here, we use the following relation for the integration of the cross-section in the unit sphere

$$\int (g_i - g'_i)\sigma d\Omega = g_i Q^{(1)} \quad \text{and} \quad \int (g_i g_j - g'_i g'_j)\sigma d\Omega = \frac{1}{2}\left(3 g_i g_j - g^2 \delta_{ij}\right) Q^{(2)}. \tag{A2}$$

The integral over the scattering angles in an electron-gas inelastic collision reads

$$\mathscr{F}^{inel,iz}_{\mathfrak{eg}}(\boldsymbol{g},\boldsymbol{G}) = \begin{pmatrix} -\frac{1}{\mu_{\mathfrak{eg}}} Q^{iz(T)}_{\mathfrak{eg}} \\ 0 \\ \left(\frac{m_{\mathfrak{e}}}{\mu_{\mathfrak{eg}}}\right)\frac{e\phi}{\mu_{\mathfrak{eg}}} Q^{(T)}_{\mathfrak{eg}} \\ \left(\frac{\mu_{\mathfrak{eg}}}{m_{\mathfrak{e}}}\right)\frac{e\phi}{\mu_{\mathfrak{eg}}} g_i (Q^{(T)}_{\mathfrak{eg}} - Q^{(1)}_{\mathfrak{eg}}) + \left(\frac{\mu_{\mathfrak{eg}}}{m_{\mathfrak{e}}}\right)\frac{e\phi}{\mu_{\mathfrak{eg}}} G_i Q^{(T)}_{\mathfrak{eg}} \\ 4\left(\frac{\mu_{\mathfrak{eg}}}{m_{\mathfrak{e}}}\right)\frac{e\phi}{\mu_{\mathfrak{eg}}} g_j G_j (Q^{(T)}_{\mathfrak{eg}} - Q^{(1)}_{\mathfrak{eg}}) + \left[\left(\frac{\mu_{\mathfrak{eg}}}{m_{\mathfrak{e}}}\right)\frac{2e\phi}{\mu_{\mathfrak{eg}}} G^2 + \left(\frac{\mu_{\mathfrak{eg}}}{m_{\mathfrak{e}}}\right)^3 \left(\frac{2e\phi}{\mu_{\mathfrak{eg}}} g^2 - \frac{2e^2\phi^2}{\mu^2_{\mathfrak{eg}}}\right)\right] Q^{(T)}_{\mathfrak{eg}} \end{pmatrix}. \tag{A3}$$

The integral over the scattering angles in an electron-electron elastic collision reads

$$\mathscr{F}^{el}_{\mathfrak{ee}}(\boldsymbol{g},\boldsymbol{G}) = \begin{pmatrix} 0 \\ 0 \\ 0 \\ \frac{1}{4}\left[g^2 G_i - 3(g_j G_j) g_i\right] \\ \frac{1}{2}\left[g^2 G^2 - 3(g_i G_i)(g_j G_j)\right] \end{pmatrix} Q^{(2)}_{\mathfrak{ee}}. \tag{A4}$$

2. Change of reference frame

In order to obtain the collision terms in a non-inertial reference frame from the solutions obtained in an inertial reference frame, we use the following expressions

$$Q_{e\alpha} = Q_{e\alpha in} - \boldsymbol{R}_{e\alpha}\cdot\boldsymbol{u}_e \tag{A5}$$

$$\boldsymbol{R}^{(hf)}_{e\alpha} = \boldsymbol{R}^{(hf)}_{e\alpha_{in}} - \frac{5}{3}Q_{e\alpha}\boldsymbol{u}_e + \frac{8}{3}\left(\boldsymbol{R}_{e\alpha}\cdot\boldsymbol{u}_e\right)\boldsymbol{u}_e + \frac{1}{2}u_e^2\boldsymbol{R}_{e\alpha} \tag{A6}$$

$$Q^{(4)}_{e\alpha} = Q^{(4)}_{e\alpha_{in}} - 4\boldsymbol{R}^{(hf)}_{e\alpha}\cdot\boldsymbol{u}_e + 10Q_{e\alpha}u_e^2 - 18u_e^2\boldsymbol{R}_{e\alpha}\cdot\boldsymbol{u}_e, \tag{A7}$$

where the subindex *in* corresponds to the source term computed in the inertial frame. As explained above, we neglect the terms of order $\mathscr{O}(u_e^2\beta_e)$ or smaller in the change of reference frame.

Appendix B: Transport coefficients

The transport coefficients are written as a function of the frequencies and the normalized contracted fourth moment as follows

$$D_e = \frac{eT_e}{m_e}\frac{\nu^{(q,3)}_{eh} + \nu^q_{ee} - \frac{5}{2}(1+\Delta_e)\nu^{(q,1)}_{eh}}{(\nu^{(q,3)}_{eh} + \nu^q_{ee})\nu^{(u,1)}_{eh} - \nu^{(q,1)}_{eh}\nu^{(u,3)}_{eh}}, \tag{B1}$$

$$\chi_e = -\frac{5}{2}\frac{(1+\Delta_e)\nu^{(q,1)}_{eh}}{\nu^{(q,3)}_{eh} + \nu^q_{ee} - \frac{5}{2}(1+\Delta_e)\nu^{(q,1)}}, \quad \alpha_e = \frac{\chi_e}{1+\Delta_e}, \tag{B2}$$

$$\mu_e = \frac{e}{m_e}\frac{\nu^{(q,3)}_{eh} + \nu^q_{ee} - \frac{5}{2}\nu^{(q,1)}_{eh}}{(\nu^{(q,3)}_{eh} + \nu^q_{ee})\nu^{(u,1)}_{eh} - \nu^{(q,1)}_{eh}\nu^{(u,3)}_{eh}} \tag{B3}$$

$$\Lambda_e = -eT_e\frac{\nu^{(u,3)}_{eh} - \frac{5}{2}\nu^{(u,1)}_{eh}}{\nu^{(q,3)}_{eh} + \nu^q_{ee} - \frac{5}{2}\nu^{(q,1)}_{eh}}, \tag{B4}$$

$$\kappa_e = \frac{5}{2}\frac{p_e e}{m_e}\frac{1+2\Delta_e}{\nu^{(q,3)}_{eh} + \nu^q_{ee} - \frac{5}{2}\nu^{(q,1)}_{eh}} \tag{B5}$$

$$\vartheta_e = \frac{5}{2}\frac{(eT_e)^2}{m_e}\frac{\Delta_e}{\nu^{(q,3)}_{eh} + \nu^q_{ee} - \frac{5}{2}\nu^{(q,1)}_{eh}}, \quad \text{and} \tag{B6}$$

$$\varkappa_e = \frac{5}{2}\frac{n_e(eT_e)^2}{m_e}\frac{1}{\nu^{(q,3)}_{eh} + \nu^q_{ee} - \frac{5}{2}\nu^{(q,1)}_{eh}} \tag{B7}$$

where the electron heavy collision frequency is computed as the sum of the contributions of ions and gas, i.e., $\nu_{eh} = \nu_{ei} + \nu_{eg}$.

The transport coefficients for the normalized fourth moment equations, Eq. (72) read

$$D_\Delta = \frac{eT_e}{m_e}\frac{\frac{14}{3}\nu_{eh}^{(u,1)} - \frac{7}{9}\nu_{eh}^{(q,1)}}{(\nu_{eh}^{(q,3)} + \nu_{ee}^{q})\nu_{eh}^{(u,1)} - \nu_{eh}^{(q,1)}\nu_{eh}^{(u,3)}} \tag{B8}$$

$$\mu_\Delta = \frac{e}{m_e}\left[\frac{\frac{2}{3}\nu_{ee}^{q}\nu_{eh}^{(q,1)}(5\nu_{eh}^{(u,1)} - 2\nu_{eh}^{(u,3)})}{\left((\nu_{eh}^{(q,3)} + \nu_{ee}^{q})\nu_{eh}^{(u,1)} - \nu_{eh}^{(q,1)}\nu_{eh}^{(u,3)}\right)^2} + \frac{\frac{74}{45}\nu_{ee}^{q} - \frac{185}{45}\nu^{(q,1)} + \frac{14}{45}\nu^{(q,3)} + \frac{4}{3}\nu^{(u,1)}}{(\nu_{eh}^{(q,3)} + \nu_{ee}^{q})\nu_{eh}^{(u,1)} - \nu_{eh}^{(q,1)}\nu_{eh}^{(u,3)}}\right] \tag{B9}$$

$$\sigma_\Delta = \frac{e}{m_e T_e}\left[\frac{\frac{4}{3}(\nu_{ee}^{q} + \nu^{(q,3)} + \nu^{(u,1)}) - \frac{10}{3}\nu^{(q,1)} - \frac{8}{15}\nu^{(u,3)}}{(\nu_{eh}^{(q,3)} + \nu_{ee}^{q})\nu_{eh}^{(u,1)} - \nu_{eh}^{(q,1)}\nu_{eh}^{(u,3)}}\right.$$
$$\left. + \frac{\frac{2}{15}\nu_{ee}^{q}(5\nu_{eh}^{(u,1)} - 2\nu_{eh}^{(u,3)})(2\nu_{ee}^{q} - 5\nu_{eh}^{(u,1)} + 2\nu_{eh}^{(q,3)})}{\left((\nu_{eh}^{(q,3)} + \nu_{ee}^{q})\nu_{eh}^{(u,1)} - \nu_{eh}^{(q,1)}\nu_{eh}^{(u,3)}\right)^2}\right] \tag{B10}$$

Appendix C: Spatially homogeneous models

1. Relaxation to a Maxwellian

We study a model that consider only the electron-electron collisions to study the relaxation to thermodynamic equilibrium ($\Delta_e = 0$). The model solves for the fourth moment, as follows

$$\frac{d\Delta_e}{dt} = -\frac{2}{15}\nu_{ee}^{\Delta}\Delta_e. \tag{C1}$$

2. Collisional cooling of electrons in a gas

We study a model that consider the collisional cooling of the electron population due to elastic and inelastic collisions. We do not consider the growth of the electron number density due to ionization, which is treated as an inelastic collision. Similarly, we do not consider electron-ion collisions. The system of equations solve for the temperature and normalized contracted fourth moment, as follows

$$\frac{dT_e}{dt} = -\frac{2}{3}\sum_{k=0}^{excit,iz} n_g K_k^{(0)}\phi_k^* + \frac{2}{3}\frac{m_e}{m_g}\nu_{eg}^{(T,2)}(T_g - T_e), \tag{C2}$$

$$\frac{d\Delta_e}{dt} = -\frac{4}{15}n_g\sum_{k=0}^{excit,iz}\left(2K_k^{(1)}\left(\frac{\phi_k^*}{T_e}\right) - K_k^{(0)}\left(\frac{\phi_k^*}{T_e}\right)^2\right) + \frac{2}{15}\frac{m_e}{m_g}\nu_{eg}^{(T,4)}\left(\frac{T_g}{T_e} - 1\right)$$
$$-\frac{2}{15}\nu_{ee}^{\Delta}\Delta_e - 2\frac{1}{T_e}\frac{dT_e}{dt}(1 + \Delta_e). \tag{C3}$$

3. Comparison to two-term Boltzmann solver

We study a model of a spatially homogeneous discharge with an imposed electric field E_x. The equations for temperature and contracted fourth-moment are solved to steady state with the following two equations,

$$\frac{dT_{\mathfrak{e}}}{dt} = -\frac{2}{3}\sum_{k=0}^{excit,iz} n_{\mathfrak{g}} K_k^{(0)} \phi_k^* + \sum_{\alpha} \frac{2}{3}\frac{m_{\mathfrak{e}}}{m_\alpha} \nu_{\mathfrak{e}\alpha}^{(T,2)} (T_\alpha - T_{\mathfrak{e}}) - \frac{2}{3} u_{\mathfrak{e}_x} E_x, \tag{C4}$$

$$\begin{aligned}\frac{d\Delta_{\mathfrak{e}}}{dt} = & -\frac{4}{15} n_{\mathfrak{g}} \sum_{k=0}^{excit,iz} \left(2K_k^{(1)} \left(\frac{\phi_k^*}{T_e}\right) - K_k^{(0)} \left(\frac{\phi_k^*}{T_e}\right)^2 \right) + \sum_{\alpha} \frac{2}{15}\frac{m_{\mathfrak{e}}}{m_\alpha} \nu_{\mathfrak{e}\alpha}^{(T,4)} \left(\frac{T_\alpha}{T_{\mathfrak{e}}} - 1\right) \\ & -\frac{2}{15}\nu_{\mathfrak{e}\mathfrak{e}}^{\Delta}\Delta_{\mathfrak{e}} - \frac{8}{15}\nu_{\mathfrak{e}\mathfrak{e}}^{q}\frac{\rho_{\mathfrak{e}} u_{\mathfrak{e}_x} q_{\mathfrak{e}_x}}{p_{\mathfrak{e}}^2} - \frac{2}{15}\frac{\rho_{\mathfrak{e}}}{p_{\mathfrak{e}}^2}\frac{e}{m_{\mathfrak{e}}} (4q_{\mathfrak{e}_x} + 10 p_{\mathfrak{e}} u_{\mathfrak{e}_x}) E_x - 2\frac{1}{T_{\mathfrak{e}}}\frac{dT_{\mathfrak{e}}}{dt}(1+\Delta_{\mathfrak{e}}),\end{aligned} \tag{C5}$$

where the velocity and heat flux are computed at every time step with the expressions in Eqs. (67)-(68), that are computed as

$$u_{\mathfrak{e}_x} = -\mu_{\mathfrak{e}} E_x \;\text{ and }\; q_{\mathfrak{e}_x} = -\mu_{\mathfrak{e}} \Lambda_{\mathfrak{e}} n_{\mathfrak{e}} E_x. \tag{C6}$$

Here, the transport coefficients are computed as a function of the collisional frequencies that depend on the energy, according to Eqs. (B3)-(B4). First, we consider a model without electron-ion collisions, i.e., $\alpha = \mathfrak{g}$ and after we include also the electron-ion collisions, i.e., $\alpha \in (\mathfrak{g}, \mathfrak{i})$.

To compare the results, we use a fluid model with a Maxwellian EEDF that solves for the balance equation for the temperature

$$\frac{dT_{\mathfrak{e}}}{dt} = -\frac{2}{3}\sum_{k=0}^{excit,iz} n_{\mathfrak{g}} K_k^{(0)} \phi_k^* + \frac{2}{3}\frac{m_{\mathfrak{e}}}{m_{\mathfrak{g}}} \nu_{\mathfrak{e}\mathfrak{g}}^{(T,2)} (T_{\mathfrak{g}} - T_{\mathfrak{e}}) - \frac{2}{3} u_{\mathfrak{e}_x} E_x, \tag{C7}$$

where the rate $K_k^{(0)}$ is computed with a Maxwellian distribution and the drift velocity is computed as

$$u_{\mathfrak{e}_x} = -\mu_{\mathfrak{e}}^{BGK} E_x \;\text{ with }\; \mu_{\mathfrak{e}}^{BGK} = \frac{e}{m_{\mathfrak{e}} \nu_{\mathfrak{h}}^{(BGK)}}. \tag{C8}$$

Here, the electron-heavy collision frequency is computed as $\nu_{\mathfrak{h}}^{(BGK)} = \nu_{\mathfrak{e}\mathfrak{g}}^{(BGK)} + \nu_{\mathfrak{e}\mathfrak{i}}^{(BGK)}$. The electron-gas collision frequency is computed as an average rate with a Maxwellian distribution at the electron temperature[18,56], as follows

$$\nu_{\mathfrak{e}\mathfrak{g}}^{(BGK)} = n_{\mathfrak{g}} < \sigma_{\mathfrak{e}\mathfrak{g}} v_e > = n_{\mathfrak{g}} n_{\mathfrak{e}} 4\pi \int_0^\infty v_e^3 Q_{\mathfrak{e}\mathfrak{g}}^{(T)} f_{\mathfrak{e}}^{(0)} dv_{\mathfrak{e}}. \tag{C9}$$

and the electron-ion collision frequency is computed as derived by Zhdanov[37] for $T_{\mathfrak{e}} \gg T_{\mathfrak{i}}$

$$\nu_{\mathfrak{e}\mathfrak{i}}^{(BGK)} = \frac{16\sqrt{\pi}}{3} n_{\mathfrak{e}} \left(\frac{m_{\mathfrak{e}}}{2eT_{\mathfrak{e}}}\right)^{3/2} \left(\frac{e^2}{4\pi\varepsilon_0 m_{\mathfrak{e}}}\right)^2 \ln\Lambda_{\mathfrak{e}\mathfrak{i}} \;\text{ with }\; \Lambda_{\mathfrak{e}\mathfrak{i}} = \frac{12\pi\varepsilon_0^{3/2} T_{\mathfrak{e}}}{e} \left(\frac{T_{\mathfrak{e}}}{n_{\mathfrak{e}} e}\right)^{1/2}. \tag{C10}$$

REFERENCES

[1]F. Taccogna and G. Dilecce, "Non-equilibrium in low-temperature plasmas," *The European Physical Journal D*, vol. 70, p. 251, Nov 2016.

[2]V. Kolobov and V. Godyak, "Electron kinetics in low-temperature plasmas," *Physics of Plasmas*, vol. 26, no. 6, p. 060601, 2019.

[3]J. P. Boeuf and L. C. Pitchford, "Two-dimensional model of a capacitively coupled rf discharge and comparisons with experiments in the gaseous electronics conference reference reactor," *Phys. Rev. E*, vol. 51, pp. 1376–1390, Feb 1995.

[4]G. Hagelaar and G. Kroesen, "Speeding up fluid models for gas discharges by implicit treatment of the electron energy source term," *Journal of Computational Physics*, vol. 159, no. 1, pp. 1–12, 2000.

[5]M. M. Becker and D. Loffhagen, "Enhanced reliability of drift-diffusion approximation for electrons in fluid models for nonthermal plasmas," *AIP Advances*, vol. 3, no. 1, p. 012108, 2013.

[6]R. E. Robson, R. D. White, and Z. L. Petrović, "Colloquium: Physically based fluid modeling of collisionally dominated low-temperature plasmas," *Rev. Mod. Phys.*, vol. 77, pp. 1303–1320, Nov 2005.

[7]L. L. Alves, "Fluid modelling of the positive column of direct-current glow discharges," *Plasma Sources Science and Technology*, vol. 16, pp. 557–569, jun 2007.

[8]G. Hagelaar and L. Pitchford, "Solving the boltzmann equation to obtain electron transport coefficients and rate coefficients for fluid models," *Plasma Sources Science and Technology*, vol. 14, pp. 722–733, 2005.

[9]A. T. del Caz, V. Guerra, D. Gonçalves, M. L. da Silva, L. Marques, N. Pinhão, C. D. Pintassilgo, and L. L. Alves, "The LisbOn KInetics boltzmann solver," *Plasma Sources Science and Technology*, vol. 28, p. 043001, apr 2019.

[10]W. Allis, "Handbuch der physik," *Springer-Verlag, Berlin*, vol. 21, pp. 383–444, 1956.

[11]R. E. Robson, R. Winkler, and F. Sigeneger, "Multiterm spherical tensor representation of boltzmann's equation for a nonhydrodynamic weakly ionized plasma," *Phys. Rev. E*, vol. 65, p. 056410, May 2002.

[12]G. K. Grubert, M. M. Becker, and D. Loffhagen, "Why the local-mean-energy approximation should be used in hydrodynamic plasma descriptions instead of the local-field approximation," *Phys. Rev. E*, vol. 80, p. 036405, Sep 2009.

[13]L. Alves, G. Gousset, and S. Vallee, "Nonequilibrium positive column revisited," *IEEE Transactions on Plasma Science*, vol. 31, no. 4, pp. 572–586, 2003.

[14]A. L. Ward, "Calculations of cathode-fall characteristics," *Journal of Applied Physics*, vol. 33, no. 9, pp. 2789–2794, 1962.

[15]J.-P. Boeuf, "Numerical model of rf glow discharges," *Phys. Rev. A*, vol. 36, pp. 2782–2792, Sep 1987.

[16]C. Busch and U. Kortshagen, "Numerical solution of the spatially inhomogeneous boltzmann equation and verification of the nonlocal approach for an argon plasma," *Phys. Rev. E*, vol. 51, pp. 280–288, Jan 1995.

[17]U. Kortshagen, C. Busch, and L. D. Tsendin, "On simplifying approaches to the solution of the boltzmann equation in spatially inhomogeneous plasmas," *Plasma Sources Science and Technology*, vol. 5, pp. 1–17, feb 1996.

[18]G. J. M. Hagelaar, G. Fubiani, and J.-P. Boeuf, "Model of an inductively coupled negative ion source: I. general model description," *Plasma Sources Science and Technology*, vol. 20, p. 015001, jan 2011.

[19]S. Lishev, L. Schiesko, D. Wünderlich, C. Wimmer, and U. Fantz, "Fluid-model analysis on discharge structuring in the RF-driven prototype ion-source for ITER NBI," *Plasma Sources Science and Technology*, vol. 27, p. 125008, dec 2018.

[20]D. Zielke, D. Rauner, S. Briefi, S. Lishev, and U. Fantz, "Self-consistent fluid model for simulating power coupling in hydrogen ICPs at 1 MHz including the nonlinear RF lorentz force," *Plasma Sources Science and Technology*, vol. 30, p. 065011, jun 2021.

[21]M. Becker and D. Loffhagen, "Derivation of moment equations for the theoretical description of electrons in nonthermal plasmas," *Advances in Pure Mathematics*, vol. 3, no. 3, pp. 343–352, 2013.

[22]S. Dujko, A. H. Markosyan, R. D. White, and U. Ebert, "High-order fluid model for streamer discharges: I. derivation of model and transport data," *Journal of Physics D: Applied Physics*, vol. 46, p. 475202, oct 2013.

[23]R. Futtersack, *Modélisation fluide du transport magnétisé dans les plasmas froids*. PhD Thesis, Universite de Toulouse III, 2014.

[24]A. H. Markosyan, S. Dujko, and U. Ebert, "High-order fluid model for streamer discharges: II. numerical solution and investigation of planar fronts," *Journal of Physics D: Applied Physics*, vol. 46, p. 475203, oct 2013.

[25]N. A. Garland, D. G. Cocks, G. J. Boyle, S. Dujko, and R. D. White, "Unified fluid model analysis and benchmark study for electron transport in gas and liquid analogs," *Plasma Sources Science and Technology*, vol. 26, p. 075003, jun 2017.

[26]H. Grad, "On the kinetic theory of rarefied gases," *Communications on Pure and Applied Mathematics*, vol. 2, no. 4, pp. 331–407, 1949.

[27]H. Struchtrup, *Macroscopic Transport Equations for Rarefied Gas Flows–Approximation Methods in Kinetic Theory*. 01 2005.

[28]G. Kremer, *An Introduction to the Boltzmann Equation and Transport Processes in Gases*. Interaction of Mechanics and Mathematics, Springer Berlin Heidelberg, 2010.

[29]M. Torrilhon and H. Struchtrup, "Regularized 13-moment equations: shock structure calculations and comparison to burnett models," *Journal of Fluid Mechanics*, vol. 513, pp. 171–198, 2004.

[30]H. Struchtrup and M. Torrilhon, "Regularization of grad's 13 moment equations: Derivation and linear analysis," *appeared in Phys. Fluids*, vol. 15, 09 2003.

[31]G. M. Kremer and W. M. Jr., "Fourteen moment theory for granular gases," *Kinetic and Related Models*, vol. 4, no. 1, pp. 317–331, 20001.

[32]H. Struchtrup, "Extended moment method for electrons in semiconductors," *Physica A Statistical and Theoretical Physics*, vol. 275, pp. 229–255, 05 2000.

[33]S.-F. Liotta and H. Struchtrup, "Moment equations for electrons in semiconductors: Comparison of spherical harmonics and full moments," *Solid-State Electronics*, vol. 44, p. 95–103, 01 2000.

[34]S. I. Braginskii, "Transport Processes in a Plasma," *Reviews of Plasma Physics*, vol. 1, p. 205, Jan. 1965.

[35]R. Balescu, "5 - the classical transport theory," in *Classical Transport* (R. Balescu, ed.), Transport Processes in Plasmas, pp. 211–276, Amsterdam: North-Holland, 1988.

[36]P. Hunana, T. Passot, E. Khomenko, D. Martínez-Gómez, M. Collados, A. Tenerani, G. Zank, Y. Maneva, M. Goldstein, and G. Webb, "Generalized fluid models of the braginskii-type," 01 2022.

[37]V. M. Zhdanov, *Transport Processes in Multicomponent Plasma*, vol. 44. CRC Press, sep 2002.

[38]R. E. Robson and K. F. Ness, "Velocity distribution function and transport coefficients of electron swarms in gases: Spherical-harmonics decomposition of boltzmann's equation," *Phys. Rev. A*, vol. 33, pp. 2068–2077, Mar 1986.

[39]K. Kumar, H. R. Skullerud, and R. E. Robson, "Kinetic theory of charged particle swarms in

neutral gases," *Australian Journal of Physics*, vol. 33, p. 343, July 1980.

[40]S. L. Lin, R. E. Robson, and E. A. Mason, "Moment theory of electron drift and diffusion in neutral gases in an electrostatic field," *The Journal of Chemical Physics*, vol. 71, no. 8, pp. 3483–3498, 1979.

[41]K. F. Ness and R. E. Robson, "Velocity distribution function and transport coefficients of electron swarms in gases. ii. moment equations and applications," *Phys. Rev. A*, vol. 34, pp. 2185–2209, Sep 1986.

[42]Z. Cai, Y. Fan, and R. Li, "Globally hyperbolic regularization of grad's moment system," *arXiv: Mathematical Physics*, 2012.

[43]I. Müller, D. Reitebuch, and W. Weiss, "Extended thermodynamics - consistent in order of magnitude," *Continuum Mechanics and Thermodynamics*, vol. 15, pp. 113–146, 04 2003.

[44]S. Chapman and T. G. Cowling, *The mathematical theory of non-uniform gases. an account of the kinetic theory of viscosity, thermal conduction and diffusion in gases*. 1970.

[45]J. Ferziger and H. Kaper, *Mathematical Theory of Transport Processes in Gases*. North-Holland Publishing Company, 1972.

[46]A. Aanesland, J. Bredin, P. Chabert, and V. Godyak, "Electron energy distribution function and plasma parameters across magnetic filters," *Applied Physics Letters*, vol. 100, no. 4, p. 044102, 2012.

[47]V. Godyak, "Rf discharge diagnostics: Some problems and their resolution," *Journal of Applied Physics*, vol. 129, no. 4, p. 041101, 2021.

[48]A. Meurer, C. P. Smith, M. Paprocki, O. Čertík, S. B. Kirpichev, M. Rocklin, A. Kumar, S. Ivanov, J. K. Moore, S. Singh, T. Rathnayake, S. Vig, B. E. Granger, R. P. Muller, F. Bonazzi, H. Gupta, S. Vats, F. Johansson, F. Pedregosa, M. J. Curry, A. R. Terrel, v. Roučka, A. Saboo, I. Fernando, S. Kulal, R. Cimrman, and A. Scopatz, "Sympy: symbolic computing in python," *PeerJ Computer Science*, vol. 3, p. e103, Jan. 2017.

[49]"Phelps database, www.lxcat.net, retrieved on april 14, 2021.."

[50]T. E. Magin, G. Martins, and M. Torrilhon, "Regularized grad equations for multicomponent plasmas," *AIP Conference Proceedings*, vol. 1333, no. 1, pp. 99–104, 2011.

[51]G. Martins, M. Kapper, M. Torrilhon, and T. Magin, "Hypersonics simulations based on the regularized grad equations for multicomponent plasmas," *6th AIAA Theoretical Fluid Mechanics Conference*.

[52]"Siglo database 2013, www.lxcat.net, retrieved on april 14, 2021.."

[53]G. Dimarco, R. Caflisch, and L. Pareschi, "Direct simulation monte carlo schemes for coulomb interactions in plasmas," *Communications in Applied and Industrial Mathematics*, vol. 1, no. 1, p. 72–91, 2010.

[54]V. Vahedi and M. Surendra, "A monte carlo collision model for the particle-in-cell method: applications to argon and oxygen discharges," *Computer Physics Communications*, vol. 87, no. 1, pp. 179–198, 1995. Particle Simulation Methods.

[55]G. J. M. Hagelaar, "Coulomb collisions in the boltzmann equation for electrons in low-temperature gas discharge plasmas," *Plasma Sources Science and Technology*, vol. 25, p. 015015, dec 2015.

[56]M. Lieberman and A. Lichtenberg, *Principles of Plasma Discharges and Materials Processing*. Wiley, 2005.